


Spring 1-1-2015

Mechanical and Moisture Absorption Properties of Biobased Gelatin Films and Composites for Construction Applications

Kristen Hess

University of Colorado at Boulder, krhe1387@colorado.edu

Follow this and additional works at: https://scholar.colorado.edu/cven_gradetds

 Part of the [Civil Engineering Commons](#), and the [Materials Science and Engineering Commons](#)

Recommended Citation

Hess, Kristen, "Mechanical and Moisture Absorption Properties of Biobased Gelatin Films and Composites for Construction Applications" (2015). *Civil Engineering Graduate Theses & Dissertations*. 25.
https://scholar.colorado.edu/cven_gradetds/25

This Thesis is brought to you for free and open access by Civil, Environmental, and Architectural Engineering at CU Scholar. It has been accepted for inclusion in Civil Engineering Graduate Theses & Dissertations by an authorized administrator of CU Scholar. For more information, please contact cuscholaradmin@colorado.edu.

Mechanical and Moisture Absorption Properties of Biobased Gelatin Films and Composites for
Construction Applications

by

KRISTEN HESS

B.S., University of Virginia, 2010

A thesis submitted to the
Faculty of the Graduate School of the
University of Colorado in partial fulfillment
of the requirement for the degree of
Master of Science
Civil Engineering
2015

This thesis entitled:
Mechanical and Moisture Absorption Properties of Biobased Gelatin Films and Composites for
Construction Applications
written by Kristen Marie Hess
has been approved for the Civil Environmental and Architectural Engineering Department

Wil V. Srubar III

Mija H. Hubler

Petros Sideris

Date_____

The final copy of this thesis has been examined by the signatories, and we find that both the content and the form meet acceptable presentation standards of scholarly work in the above mentioned discipline.

Hess, Kristen Marie (M.S., Civil Engineering)

Mechanical and Moisture Absorption Properties of Biobased Gelatin Films and Composites for Construction Applications

Thesis directed by Associate Professor Wil V. Srubar III

This study concerns the development of gelatin-based resins with improved moisture resistance and the integration of the developed resins into biobased composites for construction applications. In the U.S., 96 million tons of construction and demolition waste are landfilled each year [U.S. EPA 2009]. Therefore, there is a need for biobased construction materials that reduce reliance on non-renewable petroleum resources and biodegrade in landfills at the end of their intended service life. In this work, gelatin resins were prepared with varying concentrations of gelatin to water ratios (g/w), and 40% g/w resins were selected for techniques to improve moisture resistance by adding varying amounts of terephthalaldehyde (TPA) and wine tannin (T). The gelatin concentration of 40% g/w was selected because it demonstrated good mechanical properties, high bonding strength, and reduced moisture absorption when compared to 10%, 20%, and 30% g/w resins. The effect of concentration on the tensile mechanical properties and additives (e.g., TPA and T) on the moisture absorption properties of the gelatin based resins was investigated. Also in this work, the developed gelatin resins were used to produce two biobased composites: (1) a gelatin fiber reinforced polymer (FRP) composite and (2) a gelatin wood veneer (GWV) composite. The tensile mechanical properties and fracture surface morphology of the fully biobased gelatin-flax FRP composite were characterized and compared to FRP composites with partially biobased (e.g. gelatin-fiberglass and epoxy-flax) and fully synthetic (e.g. epoxy-fiberglass) constituents. The flexure properties of GWV composites made using gelatin resins with and without additives were

investigated in ambient, low, and high humidity conditions over time. The results from this study indicate that the tensile strength and modulus of gelatin resins exceed ACI 440.8-13 minimum requirements, and 40% g/w resin with 10% T to gelatin by weight exhibited the greatest improved moisture resistance. The data also indicate that fully biobased gelatin-flax composites exhibit similar mechanical properties compared to fully synthetic epoxy-fiberglass composites. Finally, the results show that the GWV composites maintain flexural properties in low humidity conditions after 14 days and lose flexural properties in high humidity conditions after 1 day. Based on this study, biobased gelatin resins and composites demonstrate a marked potential to be used as alternative materials in the construction industry, especially in temporary structural applications.

ACKNOWLEDGEMENTS

I would like to thank my advisor, Wil Srubar. He has supported and guided me through this process, and I am grateful for his time, teaching, and commitment. I would also like to thank Professor Petros Sideris and Professor Mija Hubler for serving on my defense committee. Finally, I would like to thank my family and friends for their unwavering encouragement, especially my parents and sister who have always inspired and supported me.

I would also like to acknowledge the Department of Civil, Environmental and Architectural Engineering, the College of Engineering and Applied Sciences, the Integrated Teaching and Learning Program and Laboratory, the Nanomaterials Characterization Facility, and the Sustainable Infrastructure Materials Laboratory (SIMLab) at the University of Colorado Boulder for making this research possible.

CONTENTS

Chapter 1.....	1
1.1 Purpose of the Study	1
1.2 Scope of the Study	1
1.2.1 Phase I: Developing Biobased Gelatin Resins.....	2
1.2.2 Phase II: Developing Biobased Gelatin Resins with Improved Moisture Resistance.....	2
1.2.3 Phase III: Developing Biobased Gelatin Fiber Reinforced Polymer (FRP) Composites ...	2
1.2.4 Phase IV: Developing Biobased Gelatin Wood Veneer (GWV) Composites	3
1.3 Arrangement of the Thesis.....	4
Chapter 2.....	5
2.1 Gelatin as a Biobased Resin.....	5
2.1.1 Interaction between Gelatin and Water	7
2.1.2 Improving the Moisture Resistance of Gelatin	9
2.2 Structural Composites for Construction	11
2.2.1 Fiber Reinforced Polymer (FRP) Composites	12
2.2.2 Engineered Wood Composites.....	14
2.3 Motivation for Biobased Composites.....	15
2.3.1 Motivation for Biobased FRP Composites	17
2.3.2 Motivation for Biobased Wood Composites	18
2.4 Applications for Biobased Composites	19
Chapter 3.....	21
3.1 Materials	21
3.2 Methods	21
3.2.1 Gelatin Film Preparation	21
3.2.2 Cross-linked Gelatin Film Preparation.....	22
3.2.3 Epoxy Film Preparation.....	25
3.2.4 Fiber Reinforced Composite Preparation	25
3.2.5 FRP Strengthened Wood Beam Preparation.....	27
3.2.6 Gelatin Wood Veneer (GWV) Composite Preparation	29
3.2.7 Breaking Force of Woven Natural Fiber Fabric	31
3.2.8 Tensile Mechanical Properties	32

3.2.9 Fiber Volume and Mass Fraction by Matrix Dissolution	34
3.2.10 Scanning Electron Microscopy	35
3.2.11 Flexural Mechanical Properties	36
3.2.12 Moisture Absorption Properties of Gelatin-based Films	40
3.2.13 Flexure Properties of GWV Composites Conditioned in High and Low Humidity	42
Chapter 4.....	44
4.1 Gelatin Resin.....	44
4.1.1 Tensile Mechanical Properties of Gelatin.....	44
4.1.2 Moisture Absorption Properties of Gelatin and Cross-linked Gelatin Resins	52
4.2 Epoxy Resin.....	56
4.2.1 Tensile Mechanical Properties	56
4.3 Woven Fabric.....	57
4.3.1 Breaking Force Properties of Light-weight Hemp, Medium-weight Hemp, and Flax.....	57
4.4 Fiber Reinforced Polymer (FRP) Composites	58
4.4.1 Tensile Mechanical Properties of G-Fl, G-Fi, E-Fl, and E-Fi	58
4.4.2 Tensile Fracture Surface Morphology of G-Fl, G-Fi, E-Fl, and E-Fi	61
4.5 FRP Composite Strengthened Wood Beams	63
4.5.1 Flexural Mechanical Properties of Poplar Strengthened with One-Ply FRP Composite ..	63
4.6 Gelatin-based Wood Veneer (GWV) Composites	65
4.6.1 Flexural Mechanical Properties	65
4.6.2 Cost Comparison of GWV Composites to Conventional Engineered Wood	67
4.6.3 Flexural Properties of GWV Composites in High and Low Humidity Conditions	68
Chapter 5.....	72
5.1 Gelatin-Based Resins	72
5.2 Gelatin-Based FRP Composites Compared to Synthetic-Based FRP Composites	73
5.3 Gelatin Wood Veneer (GWV) Composites	74
Chapter 6.....	75
References.....	77

LIST OF TABLES

Table 1: ANOVA results for tensile strength and modulus of gelatin films	47
Table 2: Minimum properties for saturating resins (ACI 440.8-13).....	49
Table 3: Volume change for 40% g/w and cross-linked 40% g/w resins	56
Table 4: Mechanical properties of resins	57
Table 5: ANOVA results for tensile strength and modulus of FRP composites	60
Table 6: Flexural mechanical properties for unreinforced poplar beam specimens	64
Table 7: Flexural mechanical properties of FRP strengthened poplar wood beam specimens	65
Table 8: Conditions in low and high humidity chambers	68

LIST OF FIGURES

Figure 1: Coil to helix transition of aqueous gelatin solution.....	7
Figure 2: Biobased resins.....	16
Figure 3: Natural fiber	17
Figure 4: Milled wood from logs	17
Figure 5: Types of construction applications.....	20
Figure 6: Gelatin resin preparation	22
Figure 7: Gelatin resin cross-linked with T	23
Figure 8: Gelatin resin cross-linked with TPA	24
Figure 9: Epoxy resin preparation.....	25
Figure 10: Gelatin based FRP composite preparation	26
Figure 11: Epoxy based FRP composite preparation.....	27
Figure 12: FRP composites in rectangular forms	27
Figure 13: Gelatin FRP strengthened poplar beam preparation.....	28
Figure 14: Epoxy FRP strengthened poplar beam preparation.....	28
Figure 15: G-Fl, G-Fi, E-Fl, and E-Fi FRP composite strengthened wood	29
Figure 16: Various species of wood veneer	30
Figure 17: GWV composite preparation.....	31
Figure 18: Process to obtain breaking force mechanical properties	32
Figure 19: Process to obtain tensile mechanical properties	33
Figure 20: Representative tensile specimens	33
Figure 21: Scanning electron microscopy (SEM).....	36

Figure 22: Process to obtain flexure mechanical properties	37
Figure 23: Plan view of flexure specimens.....	37
Figure 24: Section view of flexure specimens.....	37
Figure 25: Moisture absorption test process	41
Figure 26: Moisture absorption specimens.....	42
Figure 27: GWV composite flexure specimens humidity chambers.	43
Figure 28: Stress-strain curves for gelatin films.....	45
Figure 29: Tensile properties of gelatin films.....	46
Figure 30: Tensile strength and modulus of 30% gelatin by weight films over time.....	48
Figure 31: Tensile properties of gelatin saturating resins with comparison to ACI 440.8-13.....	51
Figure 32: Moisture content for gelatin resins.....	53
Figure 33: Moisture content for 40% g/w and cross-linked 40% g/w gelatin resins.....	55
Figure 34: Mechanical properties of natural fiber woven fabric	58
Figure 35: Tensile mechanical properties of FRP composites.....	60
Figure 36: Scanning electron microscopy images	63
Figure 37: FRP composite specimen (a) flexural set-up and (b) cross-section.	64
Figure 38: Flexural strength for gelatin based and conventional engineered wood.	66
Figure 39: Flexural modulus for gelatin based and conventional engineered wood.	66
Figure 40: Cost comparison of gelatin based and conventional engineered wood.....	68
Figure 41: Flexural properties of oak GWV composites in low humidity conditions over time..	69
Figure 42: Flexural properties of oak GWV composites in high humidity conditions over time.	70

CHAPTER 1

INTRODUCTION

1.1 Purpose of the Study

The purpose of the study is threefold: (a) to develop a biobased gelatin resin that can achieve the minimal tensile requirements as outlined by the American Concrete Institute (ACI) according to ACI 440.8-13 for saturating resins; (b) to improve the moisture resistance by preparing gelatin resins with additives (e.g., terephthalaldehyde and wine tannin); and, (c) to determine a compatible application for the developed biobased gelatin resin as a constituent of a composite (e.g., fiber reinforced polymer or engineered wood) in order to fabricate a biobased and renewable alternative to conventional composite construction materials.

1.2 Scope of the Study

The research completed within the scope of the study is organized into four phases to accomplish the threefold purpose outlined in Section 1.1. Phase I addresses part (a) of the purpose by examining the tensile mechanical properties for gelatin resins with a range of concentrations. Phase II addresses part (b) of the purpose by examining the moisture absorption properties of gelatin resins with and without additives. Phases III and IV address part (c) of the purpose by investigating two types of composite applications for the gelatin-based resin. In Phase III, the tensile mechanical properties are determined for four fiber reinforced polymer (FRP) composites and the failure surfaces are observed using scanning electron microscopy. In addition, flexural mechanical properties of prepared FRP composite strengthened poplar beams are examined. In Phase IV, gelatin, gelatin-terephthalaldehyde, and gelatin-wine tannin resins are used to laminate plies of wood veneer to produce a wood composite. The flexural properties of the gelatin wood veneer

(GWV) composite are investigated in ambient, low, and high humidity environments.

1.2.1 Phase I: Developing Biobased Gelatin Resins

The goal of Phase I was to determine the effect of concentration on the tensile mechanical properties (e.g., tensile strength and stiffness). This was accomplished by preparing gelatin resins and performing mechanical tensile testing according to ASTM D638 standard test methods using an Instron 5869 Universal Testing Machine. The selected resin concentrations were 10%, 20%, 30%, and 40% by weight of gelatin to water (g/w).

1.2.2 Phase II: Developing Biobased Gelatin Resins with Improved Moisture Resistance

The goal of Phase II was to observe the response upon exposure to moisture (e.g., moisture absorption and volume change) of gelatin, gelatin with terephthalaldehyde (TPA), and gelatin with wine tannin (T) resins. Both TPA and T have been used as additives to increase the cross-link density of gelatin-based hydrogel networks [Biscarat 2015, Peña 2010]. The moisture absorption properties (e.g., moisture content and volume change) were determined by preparing gelatin resins in a laboratory and immersing the cured resins in DI water according to a modified ASTM D5229. The moisture absorption test was conducted for gelatin resins with and without additives to compare the improvement in moisture resistance. The chosen gelatin resin concentrations were 10%, 20%, 30%, and 40% g/w. The chosen concentration to prepare gelatin resins with additives was 40% g/w. For TPA as an additive, the selected ratios were 0.25%, 0.5%, and 1% by weight of TPA to gelatin (TPA/g). For T as an additive, the selected ratios were 2.5%, 5%, and 10% by weight of T to gelatin (T/g).

1.2.3 Phase III: Developing Biobased Gelatin Fiber Reinforced Polymer (FRP) Composites

The goals of Phase III were: (1) to determine the effect of different biobased (e.g., gelatin and flax)

and synthetic (e.g., epoxy and fiberglass) resin and fiber constituents on the tensile mechanical properties (e.g., tensile strength and stiffness) and examine the fracture surface morphology of the FRP composite; and (2) to investigate the flexural properties (e.g., flexural strength and modulus) of FRP composite-strengthened wood. Goal (1) was accomplished by preparing four FRP composites and performing mechanical tensile testing according to ASTM D638 using an Instron 5869 Universal Testing Machine. The fracture surfaces from the mechanical testing were then observed using scanning electron microscopy technologies to examine the fiber-resin interface. Goal (2) was accomplished by fabricating wood flexure specimens with no reinforcement and strengthened with the four types of FRP composites in the laboratory. Then, flexure mechanical testing was performed according to ASTM D790 and using an Instron 5869 Universal Testing Machine. The selected four FRP composites were gelatin-flax (G-Fl), gelatin-fiberglass (G-Fi), epoxy-flax (E-Fl), and epoxy-fiberglass (E-Fi).

1.2.4 Phase IV: Developing Biobased Gelatin Wood Veneer (GWV) Composites

The goal of Phase IV was to investigate the flexural properties (e.g., flexural strength and stiffness) of GWV composites made using gelatin resins with and without additives and exposed to ambient, low humidity, and high humidity conditions. This was accomplished by preparing the GWV composite flexure specimens in a laboratory, conditioning the samples in the different environments, and performing mechanical flexure testing according to ASTM D790 and using an Instron 5869 Universal Testing Machine. The selected gelatin resin was 40% g/w content. The two selected gelatin resins with additives were 40% g/w content with 0.25% TPA/g addition and 10% T/g addition, respectively.

1.3 Arrangement of the Thesis

The thesis is organized into six chapters, as follows. Chapter 1 includes the purpose and outlines the scope of the study. Chapter 2 describes the background and motivation for the study. It explains the use of gelatin as a biobased resin, the structure and properties of gelatin, and previous work on improving the moisture resistance of gelatin. It also reviews fiber reinforced polymer (FRP) composites and engineered wood products, namely wood panels. Finally, Chapter 2 motivates the development of biobased composites. Chapter 3 describes in detail the materials used and experimental methods implemented for the study. Chapter 4 organizes, analyzes, and discusses the results obtained from the testing methods. Chapter 5 summarizes the accomplishment of the threefold purpose of the study and presents additional principle conclusions. Finally, chapter 6 considers possible future directions of the research.

CHAPTER 2

BACKGROUND AND MOTIVATION

2.1 Gelatin as a Biobased Resin

Animal gelatin was first used as a resin in medieval times for furniture. It was applied as a hot solution and developed strength (but never moisture resistance) upon cooling. Animal gelatin resins have been used for cabinets, furniture, instruments, paper products such as envelopes and labels, and sandpaper to bind the grit to the paper. Although animal gelatin exhibits high strength bonds between surfaces (e.g., wood and cellulose fibers), the high sensitivity to water has prevented its use for structural applications [Pizzi 1989]. The advantages of gelatin as a biobased resin include renewability, biodegradability, plasticity, adhesiveness, abundance, global availability, nontoxicity, and low cost [Gioffre 2012, Soradech 2012, Cao 2007, Leick 2009].

The annual production of gelatin in 2011 was 348.9 kilotons, and it is projected to increase to 450.7 kilotons by 2018 [Nutraceuticals World 2013]. The manufacturing process for gelatin is strictly regulated. The raw animal materials (e.g., bovine and porcine) are examined and accepted by veterinary authorities and checked and documented upon delivery to the manufacturing plant. Reputable gelatin manufacturers adhere to the Quality Management System according to ISO 9001 which complies with international regulations. Pharmaceutical grade gelatins have additional quality requirements enforced by the Food and Drug Administration, the European Pharmacopoeia, and the United States Pharmacopoeia. Test methods (e.g., bloom strength) for gelatin have been standardized by the American Organization of Analytical Chemists, the Gelatin Manufactures Institute of America, and the Gelatine Manufacturers of Europe. The standardized methods ensure reproducible and reliable results [Phillips 2011]. The annual production projection

and regulated manufacturing process suggest the continued availability and reliable consistency of gelatin, a byproduct of the agriculture industry.

Currently, gelatin-based materials are most often used in the food, packaging, pharmaceuticals, photography, and biomedical industries [Gioffre 2012, Hanani 2014, Duconseille 2015]. Recent studies show gelatin exhibits good binding and gel forming properties, and the use of gelatin in tissue adhesives is well documented in the literature [Kim 2013]. Gelatin has a high elastic modulus and tensile strength when compared to other biopolymers (e.g., starch, acaia gum) [Arvanitoyannis 2002]. These properties are highly dependent upon the gelatin source. For example, bovine and porcine gelatins have better mechanical properties than other gelatins [Chiou 2006]. Gelatin can also be manipulated during processing to produce different properties (e.g., gel strength, viscosity, setting behavior, and melting point) which depend on the polydispersity and the organization of the amino acids [Gioffre 2012]. In addition, gelatin is likely the biopolymer that is most similar to synthetic polymers due to its linear structure, limited monomer arrangement, and molecular weight distribution [Cao 2007]. Polymers from renewable animal resources, such as gelatin, have the potential to reduce the reliance on petroleum-based polymers [Peña 2010].

Gelatin, a protein found in the connective tissue of animals, is a partially degraded form of collagen (e.g., bovine and porcine) skin and bones [Khan 2010, Cao 2007, Gioffre 2012]. Gelatin is comprised mainly of the amino acids proline, glycine and 4-hydroxyproline [Peña 2010]. Commercial gelatin is derived from thermochemical degradation of collagen, which results in the disassembly of triple-helices and formation of random coils, which are stabilized by hydrogen bonds and covalent cross-linking [Gioffre 2012, Jones 2004, Bigi 2004]. In aqueous solution and at high temperature, gelatin exists in a disordered and relatively relaxed coil formation. As the solution cools to approximately 30°C and lower, gelatin becomes more ordered and develops

helical structures provided there is a sufficient concentration of gelatin in solution. At temperatures below 30°C, gelatin exists as a polymer network of both helical and random coils. Helices form at lower temperatures, but the amount never reaches 100% of the helical content that existed in the original collagen [Djabourov 2013]. A schematic of this coil to helix transition is shown in Figure 1.

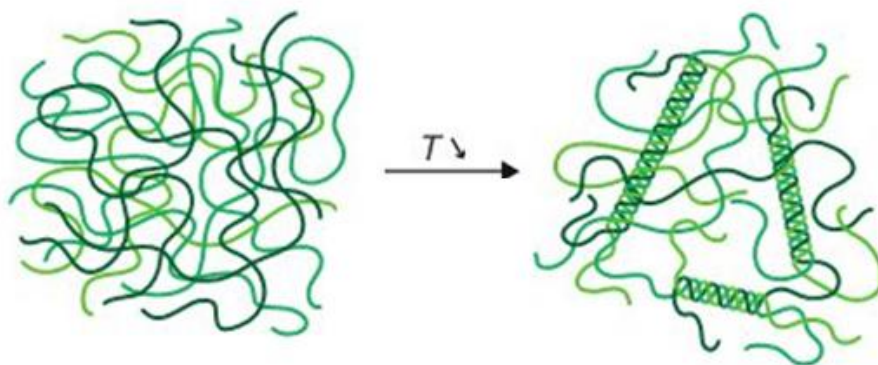


Figure 1: Coil to helix transition of aqueous gelatin solution [Djabourov 2013].

As the concentration of gelatin in the aqueous solution increases, the coils become entangled and, correspondingly, the solution becomes more viscous. It has been observed that higher gelatin concentration solutions have higher helix content. This trend suggests that nucleation, the start of helix formation, has a greater probability of occurring in concentrated solutions, but the increasingly entangled network may slow helical growth [Djabourov 2013]. This relationship between helix structure and concentration is critical because the helix structure has been attributed to the strength and other mechanical properties of the gelatin film [Gioffre 2012, Khan 2010, Cao 2007].

2.1.1 Interaction between Gelatin and Water

Gelatin hydrogels are cross-linked polymer networks that swell due to the absorption of water [Elisseeff 2008] [Ahmed 2013]. Conversely, when the hydrogel is placed in ambient conditions,

the water leaves the hydrogel causing shrinkage [Doi 2013]. Hydrophilic functional groups on the polymer chains allow for the absorption of water, while the cross-links between the chains prevent absorption [Ahmed 2013]. The gelatin network consists of chains connected by associating helices in junction zones, and the helical structures are stabilized by interchain hydrogen bonds [Bigi 2000]. The hydrogen bonds which interact with water and the polar groups of amino acids result in a brittle dry state material with high moisture absorption [Peña 2010].

The gelatin hydrogel has elastic properties and can also change in volume by absorbing the solvent, water. The difference in free energy between the dried state (i.e., the hydrogel contains no water) and the swollen state (i.e., the gel has absorbed water) is called the deformation free energy. The deformation free energy consists of the elastic energy and the mixing energy. The elastic energy is the amount of energy needed to deform the material, while the mixing energy is the energy required for the polymer network and solvent (water) to interact. If the dried gelatin hydrogel is immersed in water with no other forces acting on it, osmotic pressure will cause the gelatin network to mix with the water and expand. Simultaneously, the elastic restoring force of the gelatin network will resist the expansion. When the opposing forces are balanced, an equilibrium is reached and the gelatin network will stop absorbing water [Doi 2013].

The molecular structure of the dried state of gelatin is influenced by factors including the curing temperature, the rate of drying, and the concentration of gelatin in the initial aqueous solution. Gelatin films cast at room temperature have helical structures, and the rate of the helical formation depends on covalent bonding, molecular weight of gelatin, the presence of iminoacids, and the concentration of gelatin in solution. The amount of water bound within the helical gelatin has been reported within the literature, and the average of the literature data is 0.37 g of water per g of dry protein. The hydration of gelatin in terms of bound water can be divided into three stages:

(1) water forms intramolecular hydrogen bonds that stabilize the helical structure, (2) water is sorbed by the gelatin polar groups and directly bound to the proteins by hydrogen bonds, and (3) water is sorbed by the protein forming a polymolecular layer covering the helical structure. Water and gelatin interaction, therefore, has an influence on the formation of the helical structure. Any additional water is referred to as free water. A higher amount of free water (i.e., during gelation) results in more water-water interactions which reduces the mechanical properties (e.g., elastic modulus) [Kozlov 1983, Yakimets 2005, Yakimets 2007].

2.1.2 Improving the Moisture Resistance of Gelatin

Techniques to improve the moisture resistance of biopolymers include additives, coatings, cross-linking, bi-layering techniques, chemical treatments (e.g., acid or alkali agents), enzymatic treatment (e.g., transglutaminase), and gamma irradiation [Stevens 2002, Thakur 2015, Bourtoom 2009]. In order to improve moisture resistance of gelatin, additives such as polyols, starch, chitosan, and oligosaccharides have been incorporated into gelatin films [Peña 2010]. Gelatin films can also be cross-linked to improve their mechanical properties and, more importantly, their resistance to moisture [Biscarat 2015]. Cross-linking methods for gelatin are well documented within the literature. Cross-linking has been achieved using agents such as diisocyanates, carbodiimides, genipin, polyepoxy compounds, acyl azides, and most frequently glutaraldehyde (GTA) [Biscarat 2015, Chou 2006].

2.1.2.1 Cross-linking Gelatin with Terephthalaldehyde (TPA)

Biscarat et. al. (2015) has shown that cross-linking gelatin with TPA increases the hydrophobicity of gelatin films. TPA is a dialdehyde, like GTA, and is expected to react similarly with the amines in gelatin to form imines as a result of the Schiff base formation. In addition, other studies have shown that the Schiff base formation occurs when TPA is cross-linked with polyvinyl alcohol and

chitosan, respectively. TPA offers a nontoxic and nonvolatile alternative to other gelatin cross-linking agents. Biscarat et. al. (2015) provides the first thorough study of cross-linking gelatin with TPA.

Biscarat et. al. (2015) determined that the optimal cross-linking method is the addition of 0.005 g TPA /g gelatin to a 60°C gelatin solution. Once TPA is added, cross-linking should be completed after approximately 35 minutes. At 60°C, the gelatin polymer chains have not formed characteristic triple helices which allows for cross-linking to occur. The authors suggest that adding TPA to the gelatin solution improves moisture resistance by introducing another aromatic ring. It is also suggested that TPA reacts with the hydrophilic amine functions which prevents them from interacting with water. Biscarat et. al. (2015) found a correlation between degree of cross-linking and water absorption. The 0.005 g TPA/g gelatin had the highest degree of cross-linking at 89% and consequently has the least amount of swelling when immersed in water. Biscarat et. al. (2015) concluded that gelatin-TPA films completely immersed in water can resist dissolution for one full day. When water vapor resistance was tested in humidity chambers, the gelatin-TPA films were able to resist moisture absorption for 7 days.

2.1.2.2 Cross-linking Gelatin with Tannin

Tannins are polyphenolic compounds from vegetable tissues which have recently been investigated to replace hazardous phenols in the adhesives industry. In addition to being nontoxic, renewable, and biobased, tannin has strong affinity for the proline amino acid found in gelatin. In addition, both tannin and gelatin are soluble in water which eliminates the use of organic solvents during preparation. Gelatin and tannin are suspected to have two main interactions that improve water resistance. First, hydrogen bonds develop between the tannin hydroxyl groups and the gelatin polar groups. Second, hydrophobic interactions occur to stabilize the molecular

chemistries. For example, it is anticipated that the pyrrolidine ring of proline in gelatin has a hydrophobic interaction with the pentagalloyl glucose in tannin. It is also possible to have covalent cross-linking occur between the gelatin and tannin molecules [Peña 2010].

Peña et. al. (2010) found the addition of 10 wt% tannin (ratio of weight tannin to weight of dry gelatin) resulted in films with tensile strength and modulus of 120 and 4200 MPa, respectively. Reduced mechanical properties occurred in films with higher than 10 wt% tannin addition. In terms of moisture absorption, reduction in swelling occurred up to 10 wt% tannin which absorbed 52% less water than pure gelatin films. Higher concentrations of tannin addition did not show improved water resistance. Therefore, Peña et. al. (2010) concluded the favorable content of 10 wt% tannin addition to gelatin films resulted in strong films with higher moisture resistance than pure gelatin films.

2.2 Structural Composites for Construction

The development and advancement of the built environment depends on the capacity and availability of construction materials. Structural composites have been used since the ancient Egyptians assembled mud and straw bricks for the construction of buildings [Bai 2013]. Wood, a natural composite, has been used throughout human history as a construction material ranging from the first basic shelters to ancient ships and Chinese Temples [Rowell 2012, Bai 2013]. The fabrication of synthetic polymers in the mid 1900's led to the development of advanced polymer based composites. Initially developed for aircraft in the aerospace industry, polymer composites have found an increasing number of civil engineering applications due to their high strength-to-weight ratios [Bai 2013].

Composite materials have a wide range of applications in industries including construction,

aerospace, automotive, sports and leisure, energy, electronics, and biomedicine [Aboudi 2012, Chung 2010]. A structural composite is defined as two or more distinct materials combined to form a material system with desired and tailored properties that the constituent materials cannot obtain independently [Brigante 2013, Aboudi 2012, Chung 2010, Bai 2013]. Composites are typically comprised of a matrix material and reinforcing material. The properties of composites depend on the orientation and distribution of the constituents as well as their individual properties [Brigante 2013]. Two types of structural composite materials are (1) fiber reinforced polymer (FRP) composites and (2) engineered wood composites.

2.2.1 Fiber Reinforced Polymer (FRP) Composites

FRP composites consist of fiber reinforcement within a polymer matrix. The strength of the bond at the interface of the two constituents influences the performance of the material. The fiber reinforcement increases strength and stiffness of the composite, while the polymer matrix serves as a medium to transfer applied stresses as well as protect and secure the reinforcing fibers [Bai 2013].

FRP composites can be fabricated with many types of resins, but thermoset resins are the most common. In 2007, for example, thermoset resins were used in over 76% of manufactured FRP composites by volume [Bai 2013]. The leading thermoset polymer resins include epoxies, vinylesters, unsaturated polyesters, and phenols. In the construction industry, unsaturated polyester is the most common resin for FRP composite applications due to its low cost and ability to cure in ambient temperatures. Epoxy resins are more expensive, but they offer greater strength and stiffness as well as improved resistance to moisture and corrosion when compared to other thermoset resins. For these reasons, epoxies are chosen despite their costs for high performance applications that require durability [Bai 2013].

The first FRP composites were made of glass fibers impregnated with polymeric resins for use in aerospace applications during the thriving space exploration period in the 1960's and 1970's. The development of FRP composites in the late 1980's and through the 1990's has led to the growing acceptance of FRP composites for use in the infrastructure construction industry [Bakis 2002]. FRP composite sheets have been wrapped around structural elements (e.g., concrete and timber) and shown to improve durability of existing structures in experimental research and field applications [Bakis 2002, Lau 2001]. The use of FRP composite wrap technology for concrete cylinders has also been shown to improve the compression load capacity and stiffness. In addition, it has been shown that increasing the number of plies around the concrete cylinder increases the load capacity [Lau 2001]. The use of glass fiber FRP composites to strengthen both laminated and sawn timber elements was first studied in the 1960's. As the price of FRP composites decreased in the 1990's, the interest in researching their use to reinforce timber structures has grown [Hollaway 2008].

Plastics and FRP composites are currently used in a variety of low- and high-performance construction applications, including, piping, formwork, bridge decks, and temporary structures. The demand for materials for structural retrofit and rehabilitation has increased over the last decade due to the deteriorated state of civil infrastructure in the United States. There exists a growing need for effective, low cost retrofit techniques. Wrapping and reinforcing structural elements using FRP composites are considered a state-of-the-art technique used to improve the service life of aging and deteriorating structures [Bakis 2002, Lau 2001, Hollaway 2010]. In addition to retrofitting, the use of FRP composites for new construction projects has the potential to extend service life and improve durability of new infrastructure [Hollaway 2010, Bai 2013]. Using FRP composites to reinforce structural elements, however, has only recently been used in construction, so there is

a lack of historical data and recognized design specifications [Lau 2001]. FRP composites currently have insufficient standard test methods, material identification measures, and standards and codes which limits their use for construction applications. The lack of standardization leads to uncertainty in material performance and subsequent underutilization. [Bakis 2002, Hollaway 2010].

2.2.2 Engineered Wood Composites

Engineered wood products describe a wide range of wood based structural composites. In general, engineered wood consists of pieces of wood bonded together with adhesives using pressure and/or heat to produce panels and structural elements [Lam 2001]. The global demand for engineered wood has doubled over the past 30 years. The estimated annual consumption is 3.5 billion cubic meters, and it is projected to reach 5.2 billion cubic meters by 2050. The increasing demand is the result of factors including rising population, higher building standards, and diminishing supply of quality old growth timber [Lam 2001].

The development of wood composites was prompted by the increasing cost of timber logs and limited availability of large dimensional lumber. In addition, solid timber has disadvantages including variable properties within the cross section and limited dimensions. Wood composites can be manufactured from low grade logs (e.g., bowed or twisted) and sawmill waste material (e.g., chips or sawdust). Wood composites have more uniform and consistent properties which can be predesigned for manufacture and have higher guaranteed performance. The mechanical properties of wood composites are typically lower than natural dimensional lumber, but the consistent properties allow for a reduced safety factor. Continuous improvement of engineered wood composites is driven by technological advancement, market demand and regulations, and

the focus on minimizing the use of raw materials by developing renewable alternatives [Aguilera 2013].

Approximately 60% of produced adhesives are used for the wood panel industry, because large quantities of wood panels are used for applications including furniture, construction, and decorative and structural panels for houses [Aguilera 2013]. A successful wood panel depends equally on the adhesive and the raw wood components. Examples of wood panels include medium density fiberboard (MDF), oriented strand board (OSB), and plywood. MDF consists of randomly oriented wood fibers from thermomechanical wood pulping. The fibers are hot pressed together using thermosetting resins, and the average amount of solid resin remaining in the finished product is 11 to 14% of the cross section. OSB consists of thin wood wafers oriented in the same direction within the ply layer. The wafers are hot pressed together with thermosetting resins. The increased surface area of the wafer reduces the average amount of solid resin remaining in the finished product to 4 to 5% of the cross section. Plywood consists of layers of wood veneers hot pressed together with thermosetting adhesive resins. The resulting panel has the best strength-to-weight ratio but competes with the less expensive OSB. The adhesive resins used for wood based panels include amino plastic resins (e.g., UF, MUF, PMUF, and MUPF), phenolic resins (PF), and isocyanates (PMDI) [Aguilera 2013].

2.3 Motivation for Biobased Composites

Disposal of materials at the end of their usable life has become a growing environmental concern and has subsequently led to interest in developing of fully biobased composites that are completely biodegradable at the end of their designed service life [Netravali 2003, Netravali 2014]. A fully biobased composite is comprised of a natural reinforcing (e.g., natural fibers or wood) and a natural

polymer resin [Netravali 2014].

Figure 2 through Figure 4 show different constituents for biobased composites. Biobased resins can be derived from plants or animals, and one promising candidate for biobased construction composites is the animal-based protein, gelatin [Onusseit 2010]. Natural fibers from plants can be divided into five classifications. The bast family has the strongest fibers, and flax is a good candidate for biobased construction composites due to its high Young's modulus, accessibility, and affordability [Thakur 2013]. Milling wood provides wood materials that can be used for biobased construction composites. Veneer is a thin wood section cut using a rotary peeler for the production of engineered wood (e.g., plywood) [Aguilera 2013]. Recent research suggests that gelatin exhibits a marked potential for use in the development of biobased FRP and wood composites for construction [La Mantia 2011, Khan 2010, Aguilera 2013].

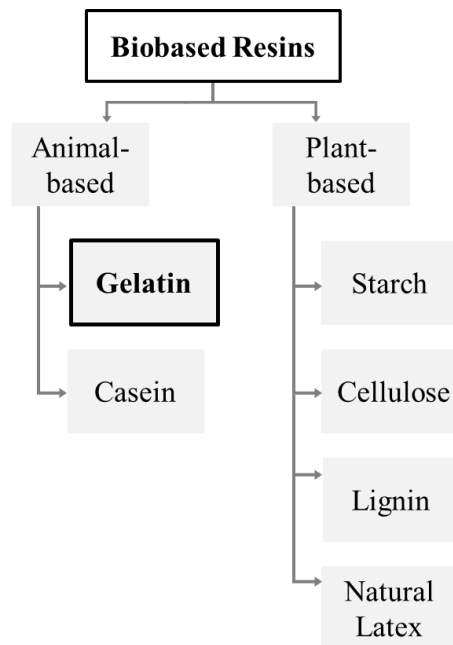


Figure 2: Biobased resins [adapted from Onusseit 2010].

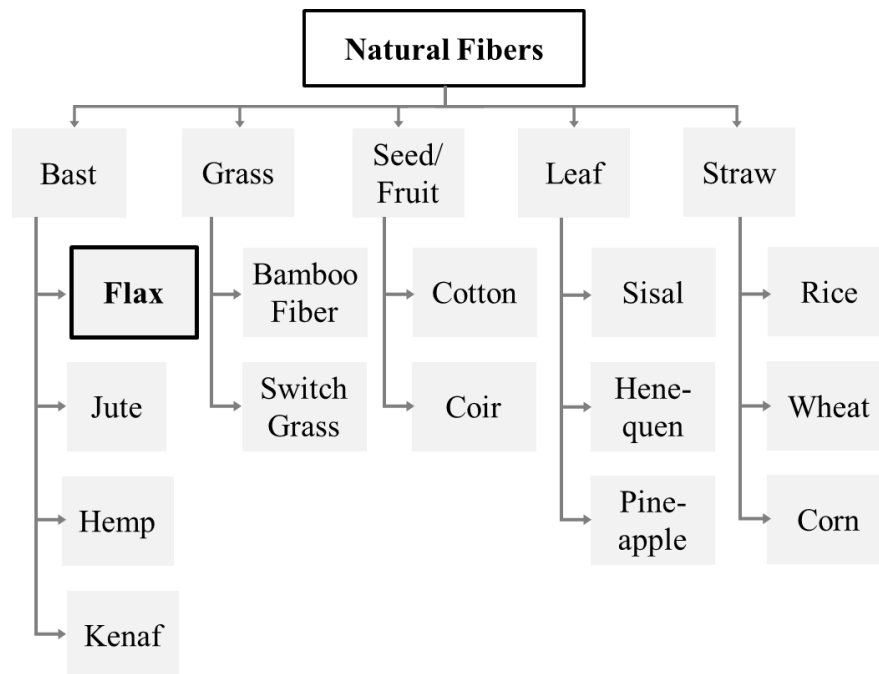


Figure 3: Natural fibers [adapted from Thakur 2013]

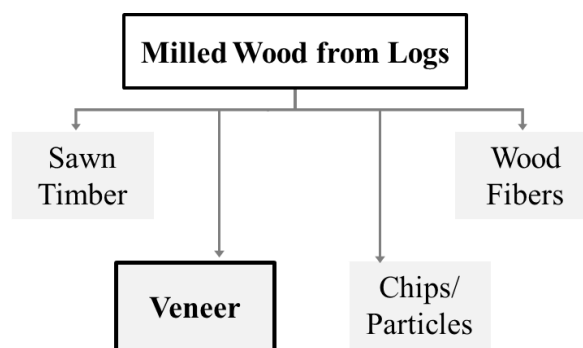


Figure 4: Milled wood from logs [adapted from Aguilera 2013].

2.3.1 Motivation for Biobased FRP Composites

Currently available FRP composites are made from non-degradable resins (e.g., epoxies, polyurethane) and high strength synthetic fibers (e.g., graphite, aramid, glass). These materials are typically petroleum-based, which is an environmental disadvantage, given that petroleum is currently consumed at a globally unsustainable rate. In addition, petroleum-based FRPs do not

readily degrade in landfills when they reach the end of their usable life [Netravali 2003, La Mantia 2011]. Finally, the use of epoxy has negative health effects including strong adhesion to human skin, skin and eye irritation, and the vapors can harm the respiratory system [Bai 2013].

Using natural fibers and biobased resins in FRP composites can alleviate the negative environmental and health impacts of petroleum-based resins and synthetic fibers [Netravali 2003]. Natural fibers have many advantages when compared to synthetic fibers, including low cost, high toughness, low density, good specific strength, renewability, recyclability, and biodegradability [Ku 2011, Khan 2010]. There exists much potential to use natural fibers in FRP composites for structural applications. For example, natural fiber reinforced composites could be used not only in retrofitting existing infrastructure, but also for constructing temporary structures in disaster relief efforts.

2.3.2 Motivation for Biobased Wood Composites

Wood composites are currently fabricated using synthetic petroleum based adhesives such as phenol formaldehyde (PF), urea formaldehyde (UF), and isocyanates [Jang 2011, Cheng 2013, Kim 2013]. The use of formaldehyde, however, has some negative effects. Formaldehyde has been identified as toxic and carcinogenic and has been shown to cause allergic reactions. Over its lifetime, formaldehyde releases volatile organic compounds (VOCs) which are known pollutants. Formaldehyde is also petroleum based; therefore, its continued use is unsustainable [Kim 2013]. In addition, a national regulation to limit the formaldehyde emissions was passed into law in July of 2010 [Jang 2011]. The negative effects of formaldehyde, the recently passed regulations, and the pressure to relieve the reliance on petroleum have motivated the development of biobased protein adhesives.

Protein based adhesives were primarily used for wood composites until they were completely replaced by the low cost and high performing synthetic adhesives [Frihart 2011, Pizzi 1989]. Protein adhesives continued to be used for interior wood bonding until the 1960s. Although synthetic adhesives dominate the current wood composite industry, the previous use of protein based adhesives suggests potential for developing them into a competitive alternative wood adhesive. Previous studies on protein based adhesives have focused on modifications and blends of cottonseed, gelatin, and most frequently soy protein [Cheng 2013, Kim 2013].

2.4 Applications for Biobased Composites

Construction material production and building operation use 40% of raw material resources, consume 40% of energy in the U.S., and release 40% of carbon dioxide emissions worldwide [Barnett 2007, U.S. DOE 2008]. Construction and demolition waste contributes 96 million tons to landfills on an annual basis [U.S. EPA 2009]. As the population grows, urbanization increases, and the infrastructure continues to age, there will be a growing demand for sustainable and resilient infrastructure. Sustainable infrastructure refers to the biorenewability and biodegradability of construction materials while considering embodied energy. Embodied energy is the energy consumed over the lifecycle of a building except during the operational phase [Dixit 2012]. Alternatively, resilient infrastructure refers to the durability and resistance to degradation (e.g., physical, chemical, mechanical, and biological) of construction material while considering service life. The trade-offs between sustainable and resilient design can be balanced by considering the application (e.g., intended use and expected lifespan) of the construction material.

Figure 5 shows a matrix that outlines construction applications. It is suggested that biobased composites could serve as alternative materials for permanent-non-structural or

temporary-structural applications, as highlighted in Figure 5. In the United States 160 million tons of waste is generated each year from construction and demolition, and 45% is from lower performance residential construction materials [U.S. EPA 2009]. Biobased composites could provide a renewable alternative material that intentionally biodegrades in a landfill at the end of its designed service life. If biobased composites are used to replace conventional materials in some capacity for feasible applications, then there is potential to contribute, in part, to the sustainability effort. The fabrication of biobased composites on a laboratory scale provides a preliminary investigation of the material properties. Successful experimental results substantiate further research and development to implement biobased composites for construction applications.

	Permanent	Temporary
Structural	Beams Columns Framing Wall Panels Roof Beams Floor Joists	Formwork Shoring Lagging Safety Rigging Scaffolding Disaster Relief Structures
Non-Structural	Partitions Doors Window Frames Flooring Cabinetry Insulation	Packaging Pallets Storage Containers Disposable Supplies Toys

Figure 5: Types of construction applications [Netravali 2014].

CHAPTER 3

MATERIALS AND METHODS

3.1 Materials

Gelatin was commercially obtained from Knox (Kraft Foods, Inc.) in granular form. The terephthalaldehyde was obtained from Sigma-Aldrich. The wine tannin powder was supplied by LD Carlson, Company and described as a dry form of premium Slovakian wine tannin from the heart of the *Castanea Sativa* chestnut tree. Two-part epoxy was obtained from Loctite with a specified strength of 24 MPa (3500 psi). Woven flax linen in a 7.5-ounce fabric was supplied by Fabric Empire. The lightweight (10 oz/yd²) and medium weight (17 oz/yd²) 100% hemp fabric was supplied by Hemp Traders. Woven 8-ounce fiberglass fabric was supplied by Plasticare. Poplar hobby board with nominal dimensions of ¼ in. x 6 in. x 48 in. were supplied by Sure-Wood Forest Products. The raw wood veneer was supplied by Sauers & Company Veneers and included mixed softwood and hardwood veneer, and white oak veneer.

3.2 Methods

3.2.1 Gelatin Film Preparation

A 300 mL beaker of water was heated to 45°C on a Corning PC-420D hotplate. Powdered gelatin, measured in percent gelatin to weight of water (g/w ratio), was added to the water and allowed to dissolve for 10 minutes under continuous stirring by a magnetic stir bar. The mixture was then poured through a strainer into a 33.7 cm x 23.5 cm rectangular form for gelation. Upon gelation, approximately 20 to 60 minutes depending on g/w ratio, the material was removed from the form and placed between two pieces of cheesecloth and two grated plates. The plates were tightly secured with ties to prevent warping. The gelatin films were cured in ambient conditions at a

temperature of $21\pm 2^\circ\text{C}$. Four classes of films with varying g/w ratios (10%, 20%, 30%, and 40%) were prepared. The method described herein is shown in Figure 6.

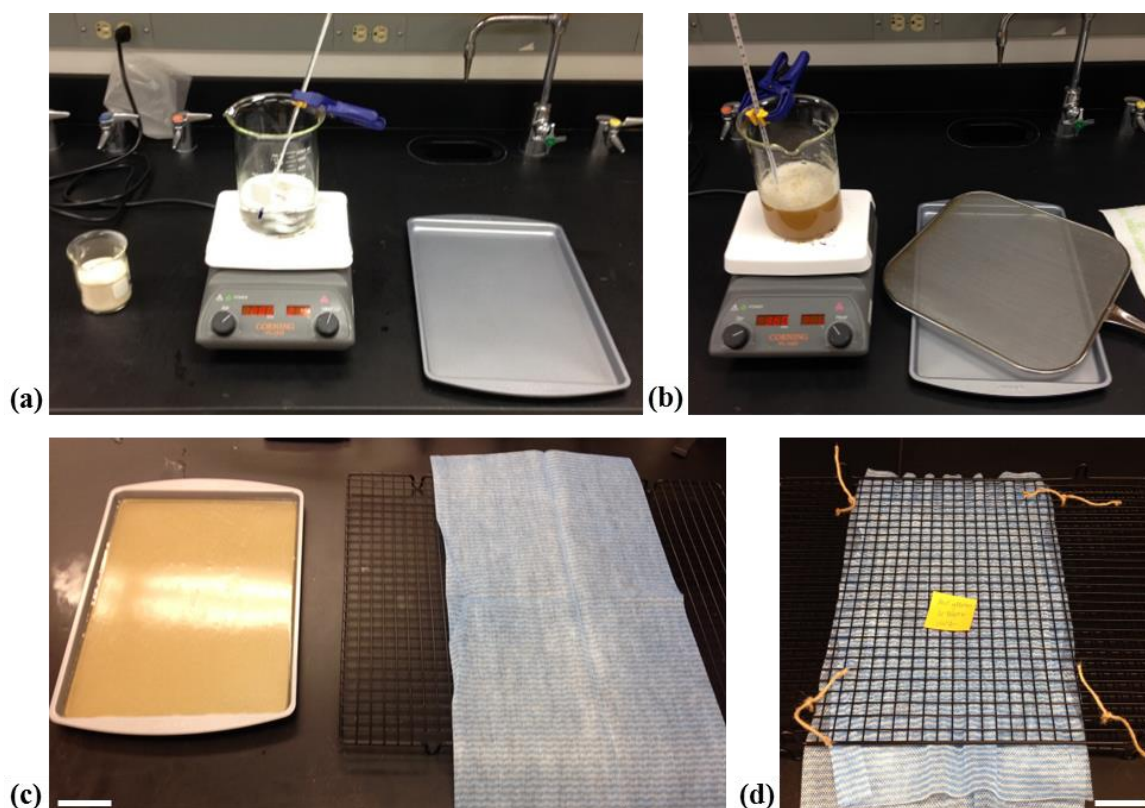


Figure 6: Gelatin resin preparation (a) beaker of water heated and powdered gelatin measured (b) solution dissolved for 10 minutes while strainer and rectangular form prepared (c) waiting for gelation to occur while grated plates and cheesecloth prepared (5cm scale bar) (d) gelled solution placed between plates and secured with ties for curing (5cm scale bar).

3.2.2 Cross-linked Gelatin Film Preparation

Cross-linking was achieved by adding the cross-linking agent (e.g., terephthalaldehyde and wine tannin) to the heated gelatin-water solution.

3.2.2.1 Gelatin Cross-linked with Wine Tannin

A 100 mL beaker of deionized (DI) water was heated to 60°C on a Corning PC-420D hotplate. Powdered gelatin, measured in percent gelatin to weight of water (g/w ratio), was added to the water and allowed to dissolve for 15 minutes under continuous stirring by a magnetic stir bar.

Powdered wine tannin (T) measured in percent weight to weight of gelatin ratios (T/g) was then added to the 60°C gelatin-water solution and allowed to mix for 45 minutes under continuous stirring by a magnetic stir bar. The mixture was then poured into a 14.6 cm x 8.3 cm rectangular form for gelation. Upon gelation, the material was removed from the form and placed between two pieces of cheesecloth and two grated plates. The plates were tightly secured with ties to prevent warping. The gelatin films were cured in ambient conditions at a temperature of $21\pm 2^\circ\text{C}$. Three classes of films with 40% g/w and varying T/g ratios (2.5%, 5%, and 10%) were prepared. The method described herein is shown in Figure 7.

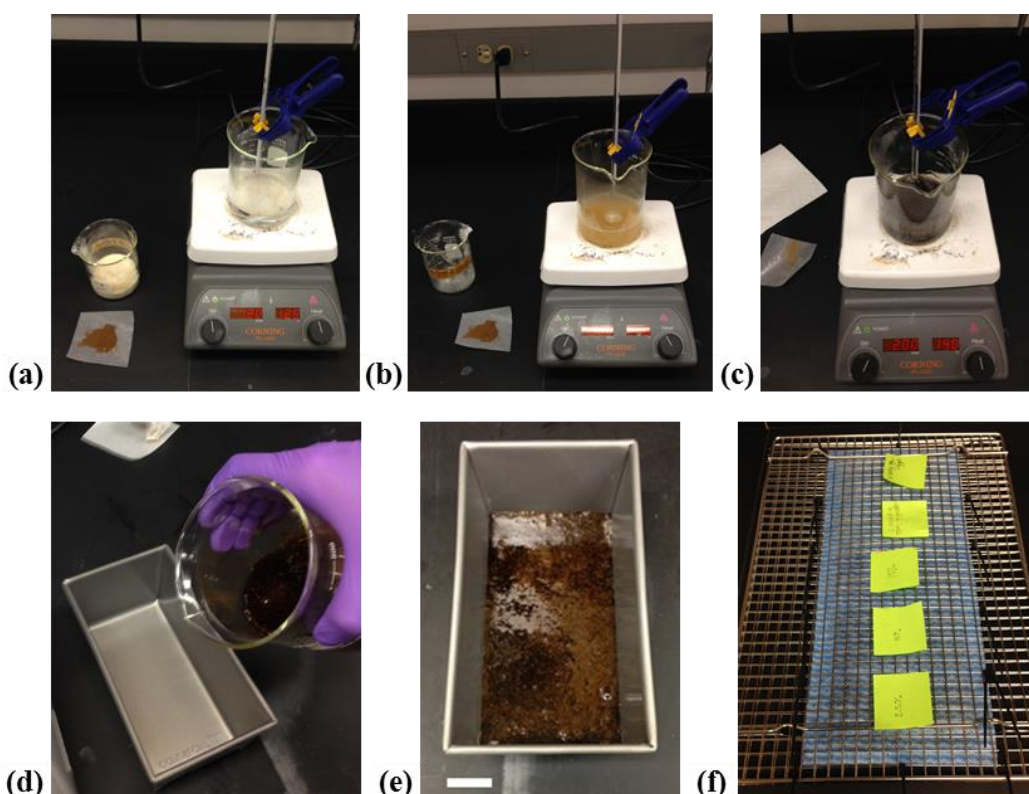


Figure 7: Gelatin resin cross-linked with T (a) water heated (b) gelatin added and dissolved (c) T added and allowed to mix (d) solution poured in rectangular form (e) gelation allowed to occur (2cm scale bar) (f) films prepared to cure.

3.2.2.2 Gelatin Cross-linked with Terephthalaldehyde

A 100 mL beaker of deionized (DI) water was heated to 60°C on a Corning PC-420D hotplate.

Powdered gelatin, measured in percent gelatin to weight of water (g/w ratio), was added to the water and allowed to dissolve for 15 minutes under continuous stirring by a magnetic stir bar. Powdered terephthalaldehyde (TPA) measured in percent weight to weight of gelatin ratios (TPA/g) was dissolved in dimethyl sulfoxide (DMSO). The subsequent solution was added to the 60°C gelatin-water solution and allowed to mix for 45 minutes under continuous stirring by a magnetic stir bar. The mixture was then poured into a 14.6 cm x 8.3 cm rectangular form for gelation. Upon gelation, the material was removed from the form and placed between two pieces of cheesecloth and two grated plates. The plates were tightly secured with ties to prevent warping. The gelatin films were cured in ambient conditions at a temperature of $21 \pm 2^\circ\text{C}$. Three classes of films with 40% g/w and varying TPA/g ratios (0.25%, 0.5%, and 1%) were prepared. The process is shown in Figure 8.

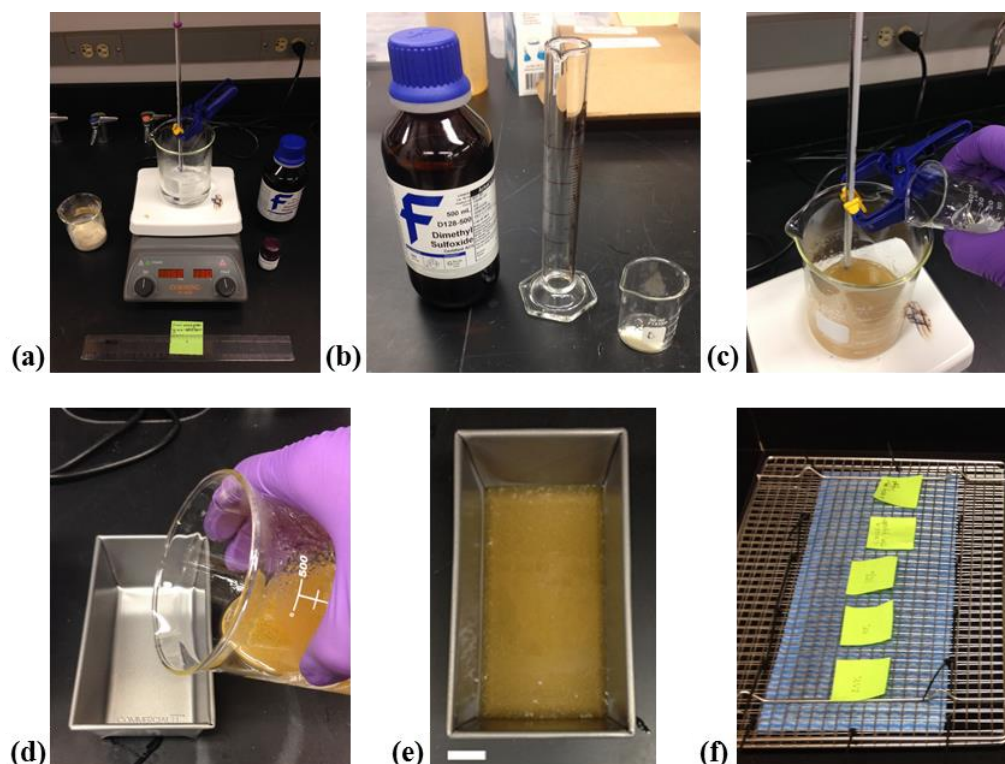


Figure 8: Gelatin resin cross-linked with TPA (a) water heated (b) dissolving TPA in DMSO (c) TPA added and allowed to mix (d) solution poured in rectangular form (e) gelation allowed to occur (2cm scale bar) (f) films prepared to cure.

3.2.3 Epoxy Film Preparation

A 33.7 cm x 23.5 cm rectangular form was coated with Blaster Dry Lube, a polytetrafluoroethylene (PTFE) lubricant spray. The powder-based Teflon lubricant was first applied to serve as a mold release for the hardened epoxy resin. Two equal parts of the epoxy resin and hardener were combined until a uniform mixture was obtained. The solution was poured into the rectangular form and allowed to cure in ambient conditions at a temperature of $21\pm 2^\circ\text{C}$. The method described herein is shown in Figure 9.

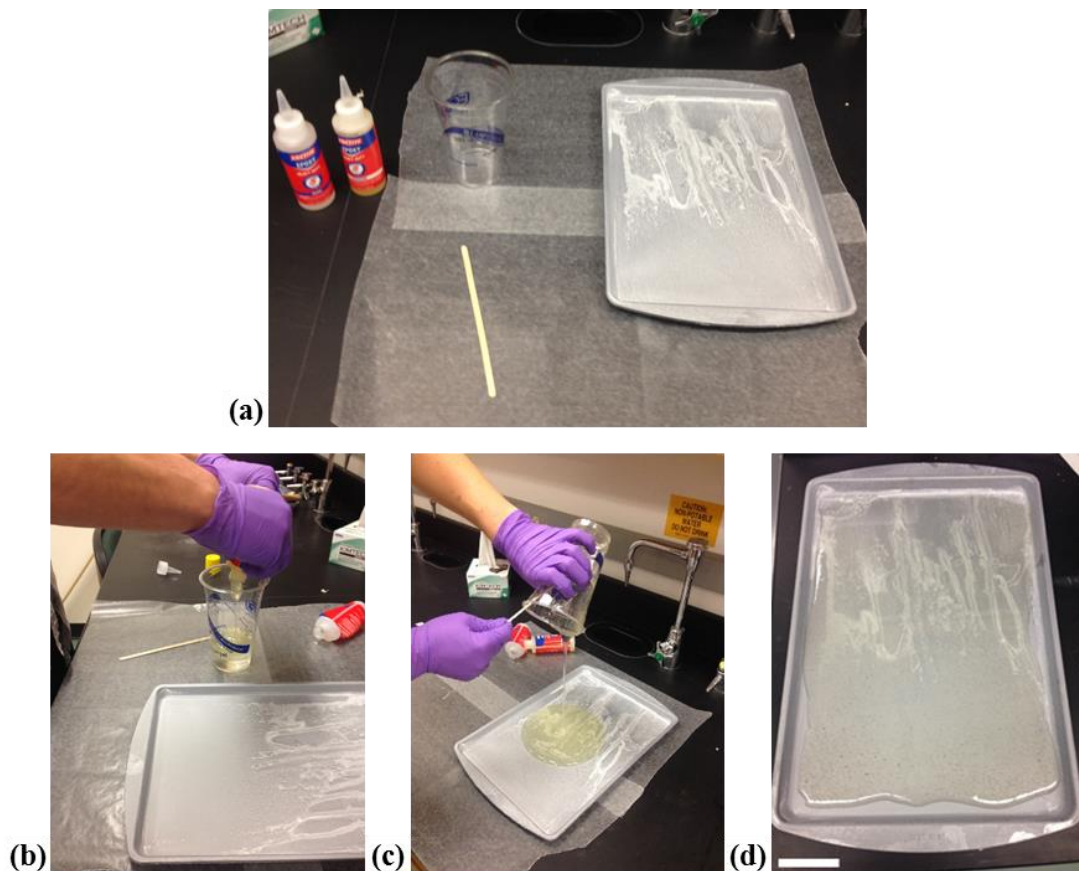


Figure 9: Epoxy resin preparation (a) rectangular form sprayed with PTFE lubricant (b) epoxy and hardener combined (c) mixture poured into form (d) solution allowed to cure in form (5cm scale bar).

3.2.4 Fiber Reinforced Composite Preparation

For this comparative study, one-ply composite specimens of gelatin-flax (G-Fl), gelatin-fiberglass

(G-Fi), epoxy-flax (E-Fl), and epoxy-fiberglass (E-Fi) were fabricated. Gelatin (30% g/w ratio) and epoxy resins were prepared as described above. Woven fabrics of flax and fiberglass were measured and cut to fit inside of a 33.7 cm x 23.5 cm rectangular form. Once the resins were poured into the rectangular forms, one sheet of woven fabric was placed on top and allowed to saturate. The fiber was then flipped over so that each side would be completely coated by the resin. Upon initial gelation (approximately 20 minutes), the gelatin-based composite material was removed from the form and placed between two grated plates, while the epoxy-based composite material was allowed to cure in the form. The plates were tightly secured with zip ties to prevent warping. Both epoxy and gelatin composites were then allowed to cure in ambient conditions at a temperature of $21\pm 2^{\circ}\text{C}$. Figure 10 shows the preparation of gelatin based FRP composites exemplified using fiberglass woven fabric and 30% gelatin resin. Figure 11 shows the preparation of epoxy based FRP composites exemplified using flax woven fabric and 2-part epoxy resin. Figure 12 shows the four (4) different FRP composites while they are in the rectangular form.

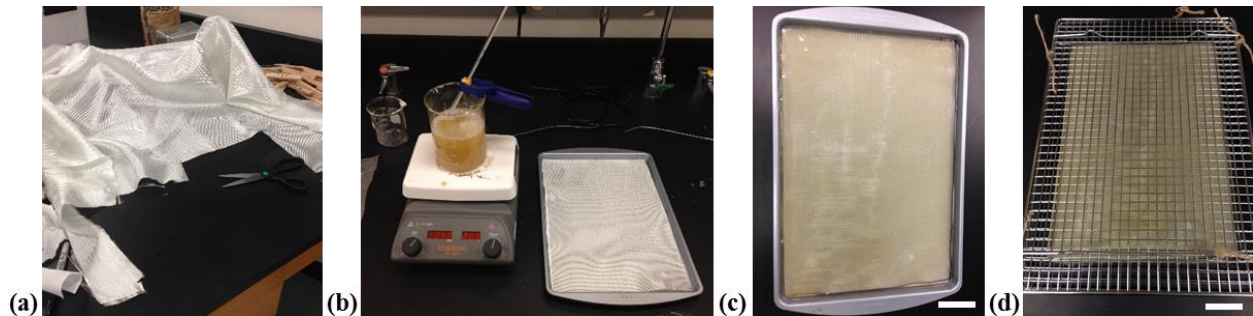


Figure 10: Gelatin based FRP composite preparation: (a) woven fabric cut to fit form (b) gelatin resin prepared (c) woven fabric saturated with gelatin resin gelling in form (5cm scale bar) (d) gelled composite placed between grated plates and secured with ties for curing (5cm scale bar).

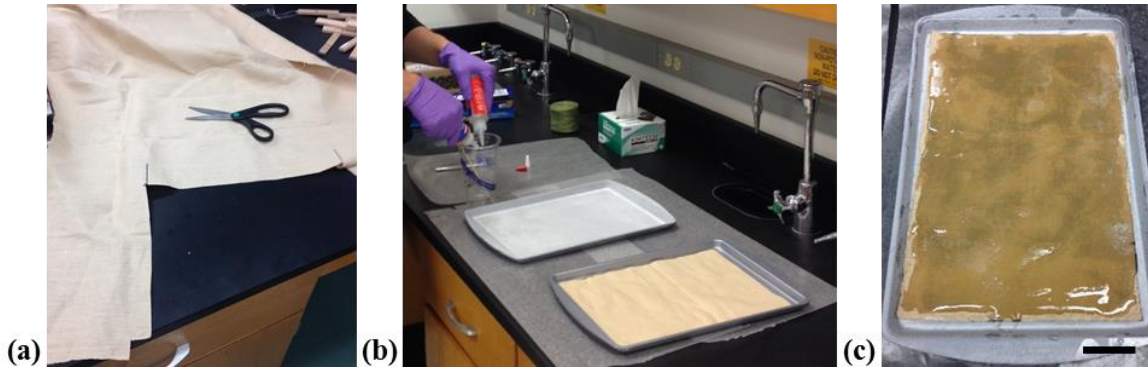


Figure 11: Epoxy based FRP composite preparation: (a) woven fabric cut to fit form (b) epoxy resin prepared (c) woven fabric saturated with epoxy resin in form for curing (5cm scale bar).

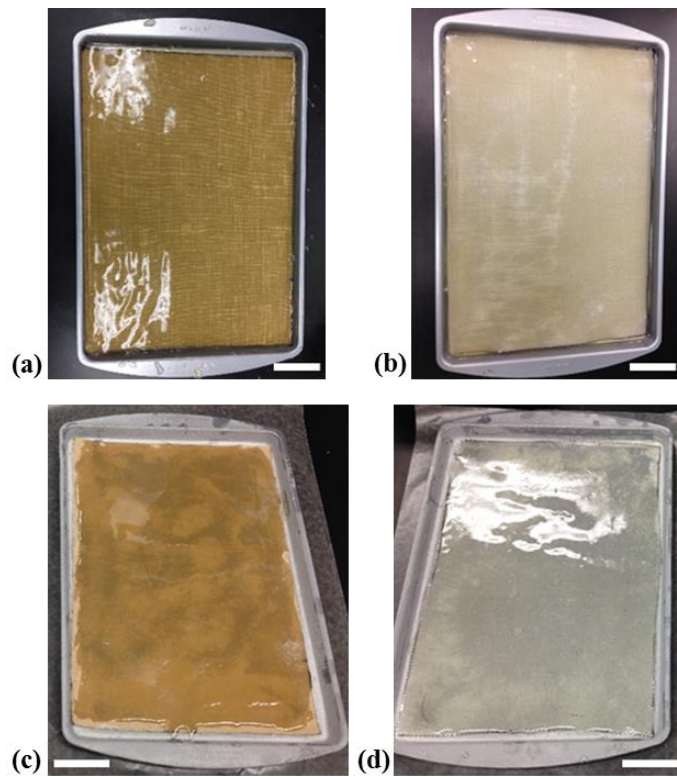


Figure 12: FRP composites in rectangular forms (a) G-Fl (b) G-Fi (c) E-Fl (d) E-Fi (5cm scale bars).

3.2.5 FRP Strengthened Wood Beam Preparation

For a comparative study, FRP strengthened wood beams were fabricated by using one-ply FRP composites of gelatin-flax (G-Fl), gelatin-fiberglass (G-Fi), epoxy-flax (E-Fl), and epoxy-fiberglass (E-Fi). Two (2) 48 in. long poplar boards were cut into two (2) 19 in. and one (1) 10 in. section. The four (4) 19 in. sections were reinforced with one-ply FRP composites. The fiber

reinforcement was cut to fit the 6 in. x 19 in. wood section. The gelatin and epoxy resins were synthesized as described in Sections 3.2.1 and 3.2.3, respectively. The woven fiber fabric was placed on top of the resin, allowed to saturate, flipped over and again allowed to saturate, and finally placed on top of the poplar wood substrate. The process for the gelatin based and epoxy based FRP composites is shown in Figure 13 and Figure 14, respectively. The FRP strengthened poplar wood, shown in Figure 15, was cured in ambient conditions at a temperature of $21\pm 2^\circ\text{C}$.

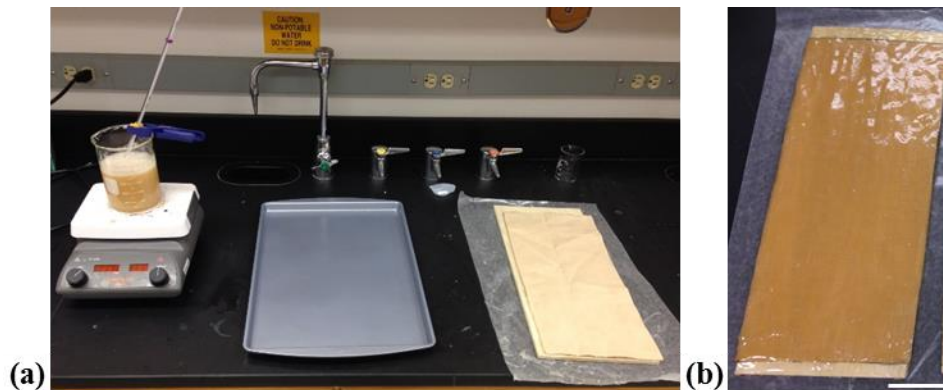


Figure 13: Gelatin FRP strengthened poplar beam preparation: (a) gelatin resin and flax woven fabric prepared for saturation (b) saturated FRP composite placed on poplar wood substrate (5cm scale bar).

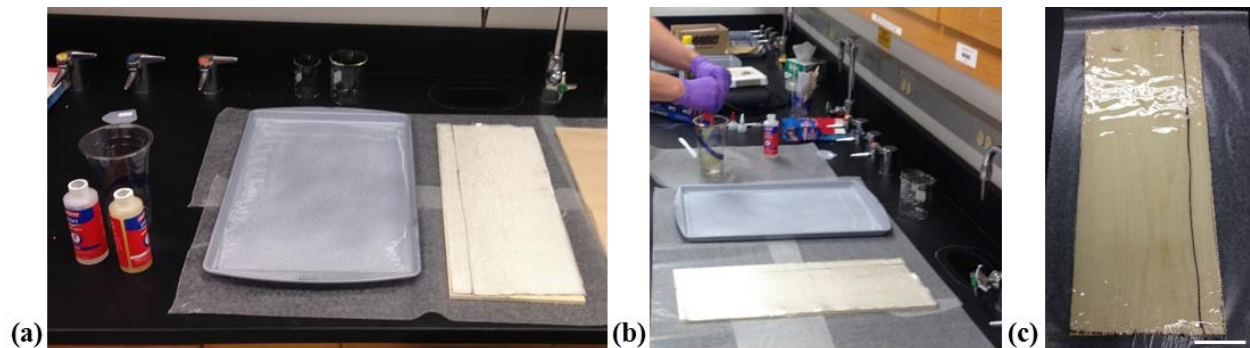


Figure 14: Epoxy FRP strengthened poplar beam preparation: (a) rectangular form sprayed with PTFE lubricant and two part epoxy and fiberglass woven fabric prepared for saturation (b) epoxy and hardener mixed (c) saturated FRP composite placed on poplar wood substrate (5cm scale bar).



Figure 15: From left to right, G-Fl, G-Fi, E-Fl, and E-Fi FRP composite strengthened wood (5cm scale bar).

3.2.6 Gelatin Wood Veneer (GWV) Composite Preparation

3.2.6.1 Softwood and Hardwood Veneer

For a comparative study, different species of wood veneer were used to fabricate the composite, including various hardwoods (Figure 16a), various softwoods (Figure 16b). The hardwood and softwood composites were balanced and symmetric and consisted of eight (8) plies of four (4) different species. The gelatin resin was prepared as described in Section 3.2.1, but heated to 60°C when applied to the wood veneer. A layer of gelatin-water solution was applied to the surface of the wood veneer. A second wood veneer was placed on top and pressed to ensure bonding over the entire surface. This process was repeated until an eight (8) ply composite was achieved. The fabricated composite was placed between two grated plates which were then tightly secured with ties to prevent warping. The composites were allowed to cure in ambient conditions at a temperature of 21±2°C. The process described herein is shown in Figure 17.

3.2.6.2 Uncross-linked and Cross-linked Gelatin-based Resins

For a comparative study, three (3) different gelatin-based resins with (1) no cross-linking agent, (2) wine tannin (T), and (3) terephthalaldehyde (TPA) were used to fabricate GWV composites using

white oak veneer. The no cross-linking agent gelatin resin had a 40% g/w ratio, the T cross-linking agent gelatin resin had a 40% g/w ratio and a 10% T/g ratio, and the TPA cross-linking agent gelatin resin had a 40% g/w ratio and a 0.25% TPA/g ratio. The resins were prepared as described in Sections 3.2.1 (but heated to 60°C for 15 minutes), 3.2.2.1, and 3.2.2.2, respectively. The GWV composites were balanced and symmetric and consisted of eight (8) plies of the same white oak wood species. They were fabricated using the process described in Section 3.2.6.1 and shown in Figure 17.

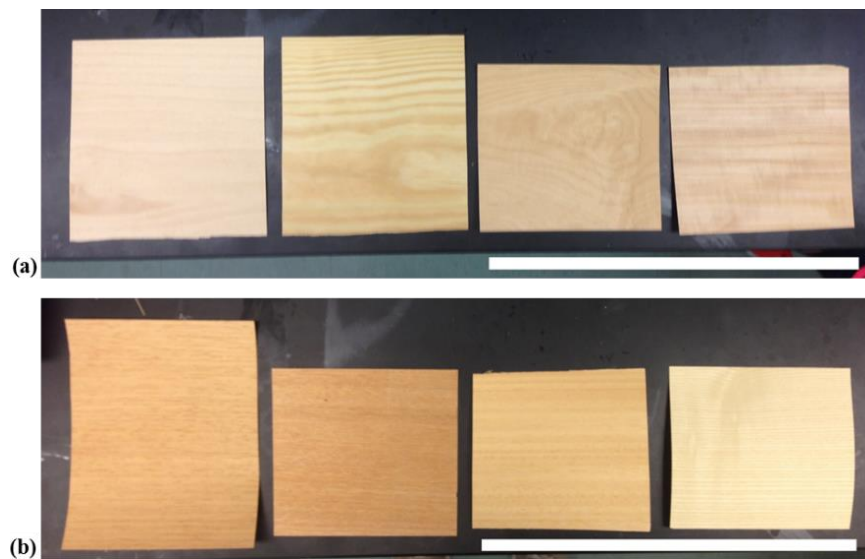


Figure 16: Various species of wood veneer (a) softwood (b) hardwood (30cm scale bars).

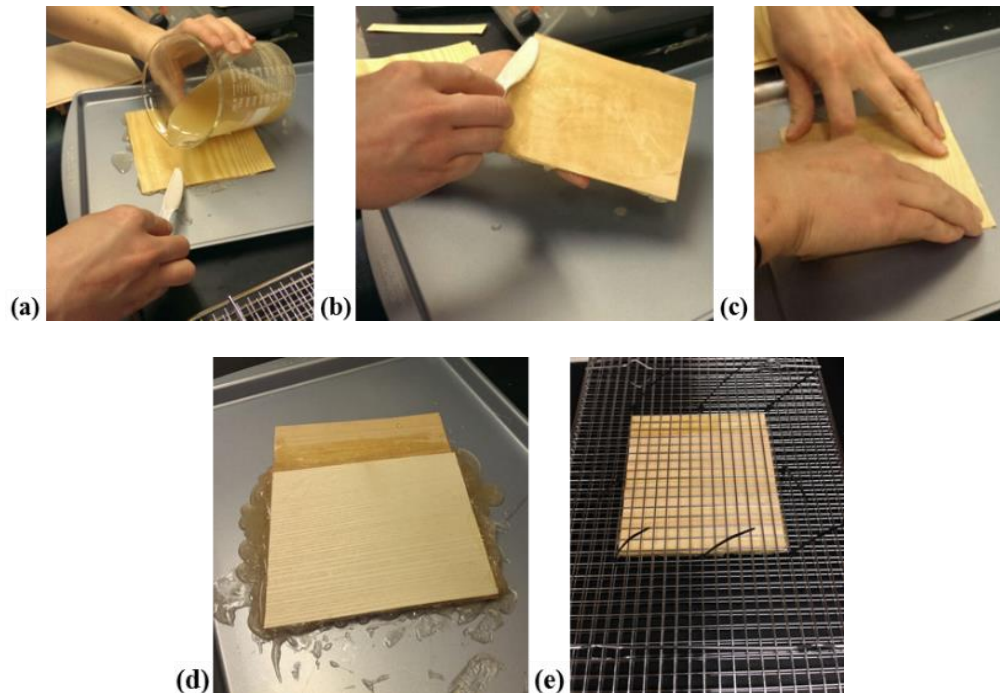


Figure 17: GWV composite preparation: (a) prepared 40% gelatin resin added to veneer (b) resin spread evenly over veneer surface (c) another veneer added to coated surface and pressed (d) fabricated 8-ply composite (e) composite placed between grates and secured with ties for curing.

3.2.7 Breaking Force of Woven Natural Fiber Fabric

For a comparative study, different woven natural fiber fabrics were tested to determine the breaking force of each material. The woven fabrics included light-weight hemp, medium-weight hemp, and flax. According to ASTM D5035, the breaking force specimens were cut into approximately 25 mm by 150 mm strips, and the fibers were oriented parallel and perpendicular to the to the direction of the applied force. The breaking force of each natural fiber woven fabric was determined according to ASTM D5035 standard test methods. The mechanical testing was conducted using an Instron 5869 Universal Testing Machine and a displacement-controlled rate of 0.5 mm/s. For each parameter of the study, at least five (5) replicate specimens were tested. The process described herein is shown in Figure 18.

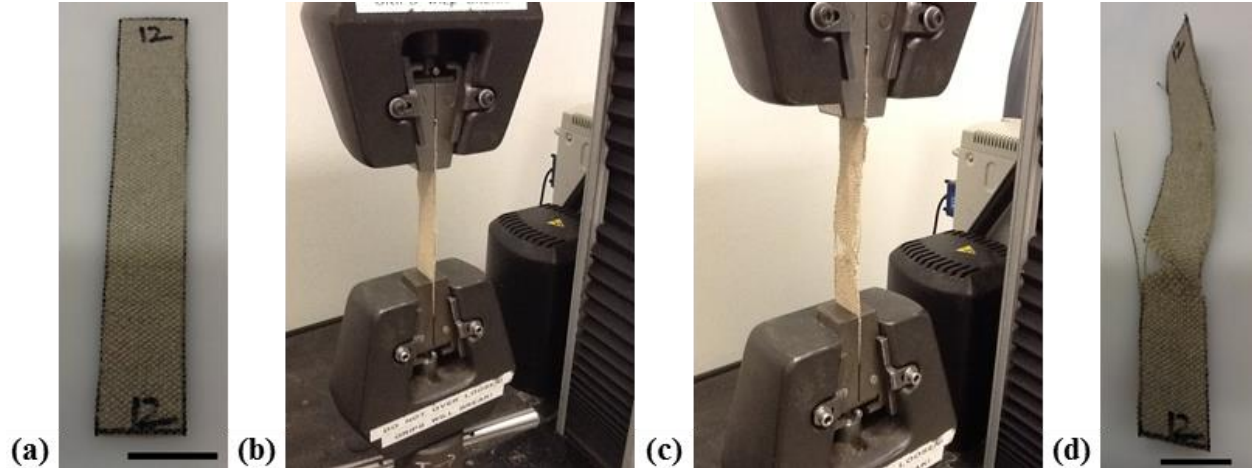


Figure 18: Process to obtain breaking force mechanical properties: (a) representative woven fabric specimen (25mm scale bar) (b) specimen in the Instron grips ready to test (c) specimen tested to failure (d) representative failed specimen (25mm scale bar).

The breaking force was calculated by determining the maximum applied load, P_{max} , carried by the specimen, and the breaking force per mm was computed using the following equation:

$$\text{Breaking Force per mm} = \frac{P_{max}}{t} \quad \text{Eq. 1}$$

where P_{max} is the maximum applied load (N), and t is the thickness (mm) of the woven fabric sample.

3.2.8 Tensile Mechanical Properties

After the curing of films and composite plates, tensile test specimens were laser cut according to the dimensions outlined in ASTM D638 using an Epilog Legend 36EXT laser system. The tensile properties of the gelatin films and fiber composites were determined according to ASTM D638 standard test methods. Using a displacement-controlled rate of 5 mm/min as specified in ASTM D638, the tension tests were conducted using an Instron 5869 Universal Testing Machine and an Epsilon Technology Corp axial extensometer model 3542 with a 1.0 inch gauge length. For each

parameter of the study, at least five (5) replicate specimens were tested. The process described herein is shown in Figure 19, and representative tensile specimens are shown in Figure 20.

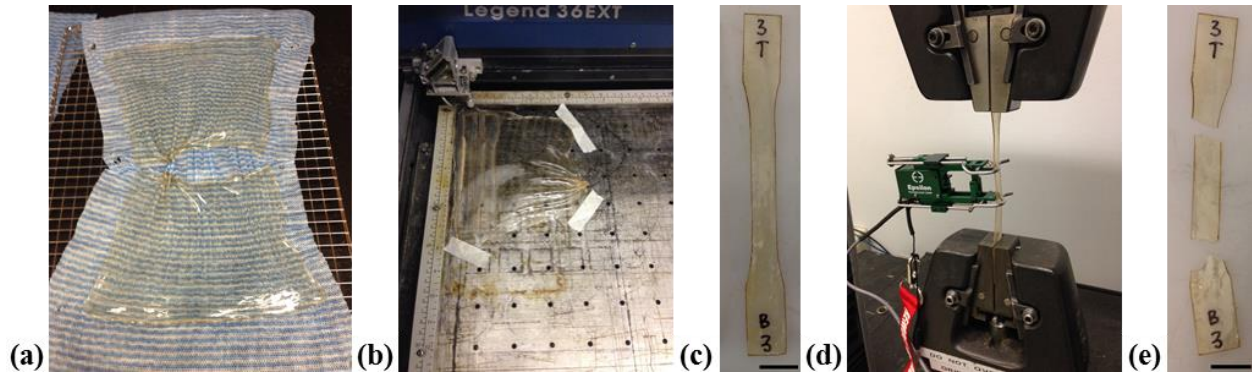


Figure 19: Process to obtain tensile mechanical properties (a) cured gelatin film (20mm scale bar) (b) laser cutting gelatin film into tensile specimens (c) representative tensile specimen (d) specimen in the Instron grips with extensometer ready to test (e) specimen tested to failure (20mm scale bar).

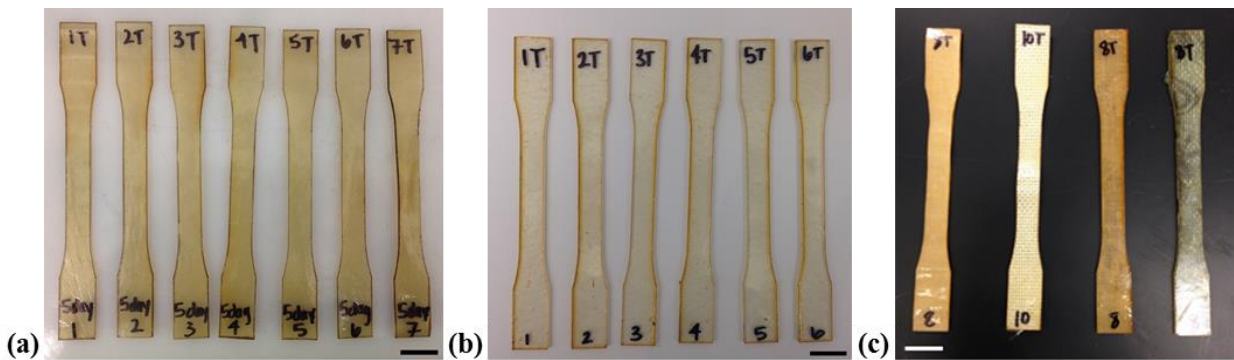


Figure 20: Representative tensile specimens (20mm scale bars) (a) 30% gelatin films cured for 5 days (b) 2-part epoxy film (c) from left to right, G-Fl, G-Fi, E-Fl, and E-Fi FRP composites.

Tensile strength, elongation-to-break, and tensile modulus were determined for each specimen. The maximum tensile strength (MPa), $\sigma_{t\ max}$, was calculated using the following equation:

$$\sigma_{t\ max} = \frac{P_{max}}{A} \quad \text{Eq. 2}$$

where P_{max} is the maximum applied load (N) and A is the cross-sectional area (mm^2) within the gauge length of the specimen where fracture occurs. The elongation-at-break (mm/mm), ϵ_u , occurs

in conjunction with the maximum tensile strength and is determined from the data collected by the extensometer. The tensile modulus (MPa), E_t , is defined by the following relationship:

$$E_t = \frac{\sigma_t}{\varepsilon} \quad \text{Eq. 3}$$

where σ_t is the tensile stress (MPa) and ε is the strain (mm/mm). The tensile modulus, E_t , was computed by determining the slope of a linear regression based on the stress-strain data between 10% and 40% of the maximum tensile stress and corresponding strain.

3.2.9 Fiber Volume and Mass Fraction by Matrix Dissolution

The gelatin and epoxy fiber reinforced composites described in Section 3.2.4 and 30% gelatin and epoxy resin described in Sections 3.2.1 and 3.2.3, respectively, were laser cut after fully cured using an Epilog Legend 36EXT laser system into 18mm x 18mm squares. Three (3) samples of each FRP composite and resin were tested. The samples were weighed and dimensions to obtain mass and volume of the composites and resins. The epoxy-based FRP samples were immersed in acetone solution for 8 days to remove the bulk of the epoxy resin. The epoxy-based FRP samples were then immersed in 50°C acetone solution and subjected to continuous stirring for 10 minutes using a Corning PC-420D hotplate. After 10 minutes, the epoxy-based FRP sample was extracted from acetone solution, the epoxy mechanically removed, and the sample was placed back into the 50°C acetone solution for an additional 10 minutes. Then, the remaining fiber from the epoxy-based FRP sample was placed on a drying rack. The gelatin-based FRP samples were immersing in 60°C water solution subjected to continuous stirring for 20 minutes using a Corning PC-420D hotplate. The remaining fiber was extracted from the water solution, blotted, and placed on a drying rack. All of the remaining fiber samples were weighed and placed in the oven at 42°C for 24 hours to drive off any remaining solution. The final fiber weights after oven drying were recorded and

used to determine the mass and volume fractions of the respective FRP composites.

The fiber mass fraction, W_f , was computed according to the following equation, since the weight of the composite and fibers were experimentally determined.

$$W_f = \frac{w_f}{w_c} \quad \text{Eq. 4}$$

where w_f is the mass of the fiber (g) and w_c is the weight of the composite (g). The mass of the resin matrix (g), w_m , was determined according to the following equation:

$$w_m = w_c - w_f \quad \text{Eq. 5}$$

The volume of the resin matrix (cm^3), v_m , was determined using the density of the resin found from the resin samples and computed according to the following equation:

$$v_m = \frac{w_m}{\rho_m} \quad \text{Eq. 6}$$

where w_m is the mass of the resin matrix (g) and ρ_m is the density of the resin matrix (g/cm^3). The volume of the fiber (cm^3), v_f , was found using the following equation:

$$v_f = v_c - v_m \quad \text{Eq. 7}$$

where v_c is the volume of the composite (cm^3) and v_m is the volume of the resin matrix (cm^3).

Finally, the fiber volume fraction, V_f , can be computed according to the following equation:

$$V_f = \frac{v_f}{v_c} \quad \text{Eq. 8}$$

3.2.10 Scanning Electron Microscopy

The fracture surfaces of the tensile-tested FRP composites were investigated using scanning electron microscopy. The samples were laser cut from the fractured specimens using an Epilog Legend 36EXT laser system. Then, the samples were sputter-coated with gold, as shown in Figure 21a, before examination in a JEOL JSM 6480LV scanning electron microscope (SEM), shown in

Figure 21b. The specimens were observed in a nitrogen atmosphere under vacuum with a voltage of 10 kV.

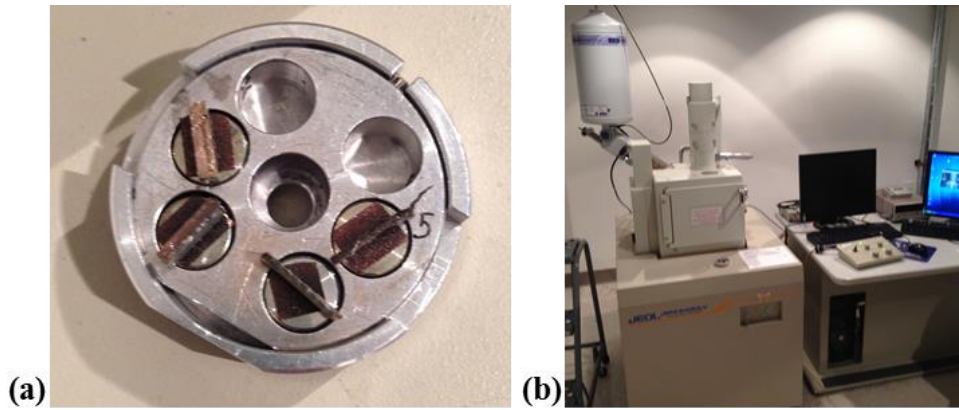


Figure 21: Scanning electron microscopy (SEM) (a) sputter coated fracture surface of FRP composite samples on the SEM stage (b) the SEM apparatus.

3.2.11 Flexural Mechanical Properties

After curing was complete, the flexure specimens for the FRP strengthened wood and the gelatin wood veneer (GWV) composite were cut using a bandsaw to dimensions specified by ASTM D790. The flexure properties of specimens were determined according to ASTM D790 standard test methods. The three-point bend flexure tests were conducted using an Instron 5869 Universal Testing Machine with LabVIEW software. For each parameter of the study, at least three (3) specimens were tested in order to record a mean value and standard deviation. The process described herein is shown in Figure 22. The flexure specimens are shown from plan and section views in Figure 23 and Figure 24, respectively.

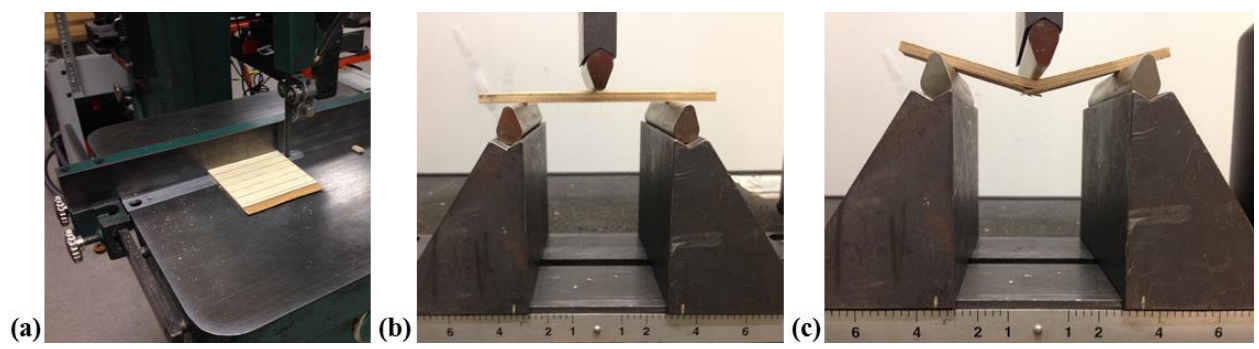


Figure 22: Process to obtain flexure mechanical properties (a) use bandsaw to cut specimens to applicable dimensions (b) specimen in the Instron three-point set up (c) specimen tested to failure.

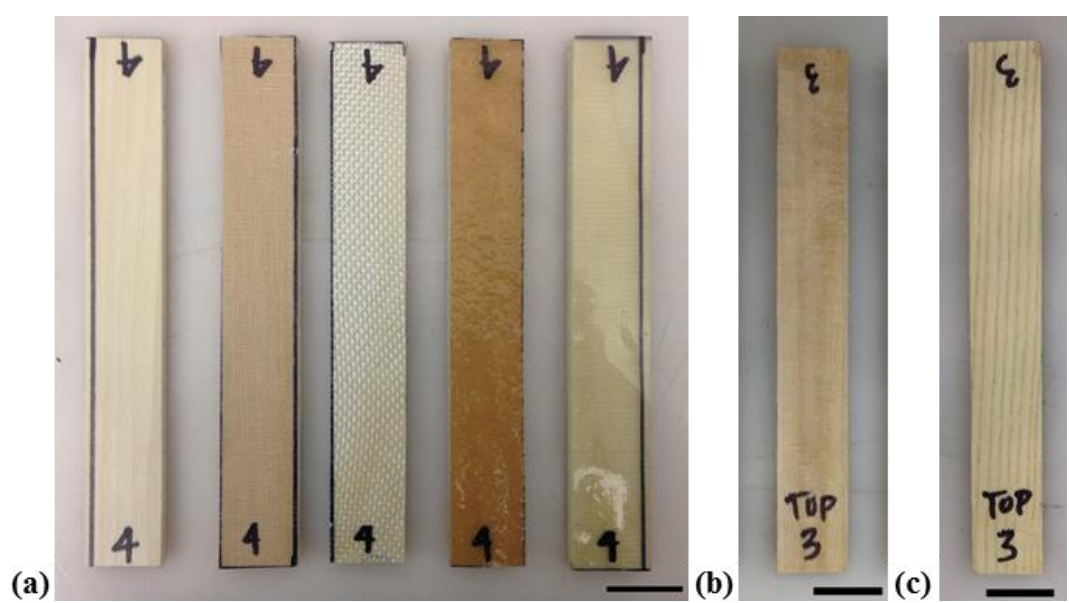


Figure 23: Plan view of flexure specimens (a) from left to right, poplar, G-Fl, G-Fi, E-Fl, E-Fi strengthened poplar (25mm scale bar) (b) softwood GWV composite (18mm scale bar) (c) hardwood GWV composite (18mm scale bar).

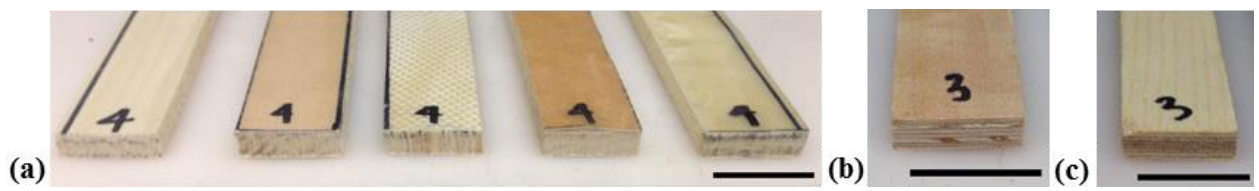


Figure 24: Section view of flexure specimens (a) from left to right, poplar, G-Fl, G-Fi, E-Fl, E-Fi strengthened poplar (25mm scale bar) (b) softwood GWV composite (18mm scale bar) (c) hardwood GWV composite (18mm scale bar).

Flexural strength and flexural modulus was calculated for each poplar specimen and each GWV composite specimen. The maximum flexural strength (MPa), $\sigma_{f\ max}$, was calculated according to the following equation:

$$\sigma_{f\ max} = \frac{3 P_{max} L}{2 b h^2} \quad \text{Eq. 9}$$

where P_{max} is the maximum applied load (N), L is the span length (mm), b is the width (mm) of the specimen, and h is the height (mm) of the specimen. The flexural modulus (MPa), E_f , was calculated according to the following equation:

$$E_f = \frac{C L^3}{4 b h^3} \quad \text{Eq. 10}$$

where C is the slope of a linear regression based on the load-displacement data between 10% and 40% of the maximum applied load and corresponding displacement.

Flexural strength and modulus were calculated for each FRP strengthened poplar wood specimen based on the method of transformed sections. The transformation factor, n , was calculated according to the following equation:

$$n = \frac{E_{FRP}}{E_w} \quad \text{Eq. 11}$$

where E_{FRP} is the tensile modulus (MPa) of the fiber reinforced polymer material calculated as described in Section 3.2.8 and E_w is the flexural modulus (MPa) of the poplar wood specimen as described above. The neutral axis (mm), \bar{y} , of the corresponding transformed section with equivalent wood was calculated according to the following equation:

$$\bar{y} = \frac{\left(\frac{1}{2}h_{FRP}\right)n A_{FRP} + \left(h_{FRP} + \frac{1}{2}h_w\right)A_w}{n A_{FRP} + A_w} \quad \text{Eq. 12}$$

where h_{FRP} is the height (mm) of the FRP material, A_{FRP} is the area (mm²) of the FRP material, h_w is the height (mm) of the wood material, and A_w is the area (mm²) of the wood material. The

moment of inertia (mm^4), I , about the neutral axis (mm), \bar{y} , is then calculated based on the parallel axis theorem according to the following equation:

$$I = \left[\frac{1}{12} b h_w^3 + A_w d_w^2 \right] + \left[\frac{1}{12} n b h_{FRP}^3 + n A_{FRP} d_{FRP}^2 \right] \quad \text{Eq. 13}$$

where b is the width (mm) of the specimen, d_w is the distance (mm) from the centroid of the wood material to the neutral axis, and d_{FRP} is the distance (mm) from the centroid of the FRP material to the neutral axis. The maximum moment (N-m), M_{max} , in the beam specimen is calculated according to the following equation:

$$M_{max} = \frac{P_{max} L}{4} \quad \text{Eq. 14}$$

where P_{max} is the maximum applied load (N), and L is the span length (mm). The maximum flexural strength (MPa) in the wood and FRP materials at the bottom, interface, and top of the cross-section are calculated according to the following equations:

$$\sigma_{FRP \text{ bottom}} = \frac{n M_{max} d_b}{I} \quad \text{Eq. 15}$$

$$\sigma_{FRP \text{ interface}} = \frac{n M_{max} d_i}{I} \quad \text{Eq. 16}$$

$$\sigma_w \text{ interface} = \frac{M_{max} d_i}{I} \quad \text{Eq. 17}$$

$$\sigma_w \text{ top} = \frac{M_{max} d_t}{I} \quad \text{Eq. 18}$$

where d_b is the distance (mm) from the neutral axis to the bottom of the beam specimen cross-section, d_i is the distance (mm) from the neutral axis to the interface of the two materials within the beam specimen cross-section, and d_t is the distance (mm) from the neutral axis to the top of beam specimen cross-section. The flexural modulus (MPa), E_f , of the FRP strengthened poplar wood specimens was calculated according to the following equation:

$$E_f = \frac{C L^3}{48 I} \quad \text{Eq. 19}$$

where C is the slope of a linear regression based on the load-displacement data between 10% and 40% of the maximum applied load and corresponding displacement.

3.2.12 Moisture Absorption Properties of Gelatin-based Films

The moisture absorption properties of four (4) classes of gelatin films with varying g/w ratios (10%, 20%, 30%, and 40%), three (3) classes of 40% g/w films with varying T/g ratios (2.5%, 5%, 10%), and three (3) classes of 40% g/w films with varying TPA/g ratios (0.25%, 0.5%, and 1%) were determined according to modified ASTM D5229 standard test methods. The gelatin films were prepared as described above. After curing for 3 days in ambient conditions, the films were placed in an oven at 60°C to extract unbound water. The specimens were weighed using a Mettler Toledo XS105 DualRange scale at different time intervals until weight loss was negligible. The gelatin films were then laser cut into 15 mm by 15 mm squares using an Epilog Legend 36EXT laser system. At least three (3) specimens for each ratio were tested in order to record a mean value and standard deviation. After laser cut, the specimens were weighed and measured using calipers then immersed completely in water with a temperature of $21 \pm 1^\circ\text{C}$. Figure 25 shows the process.

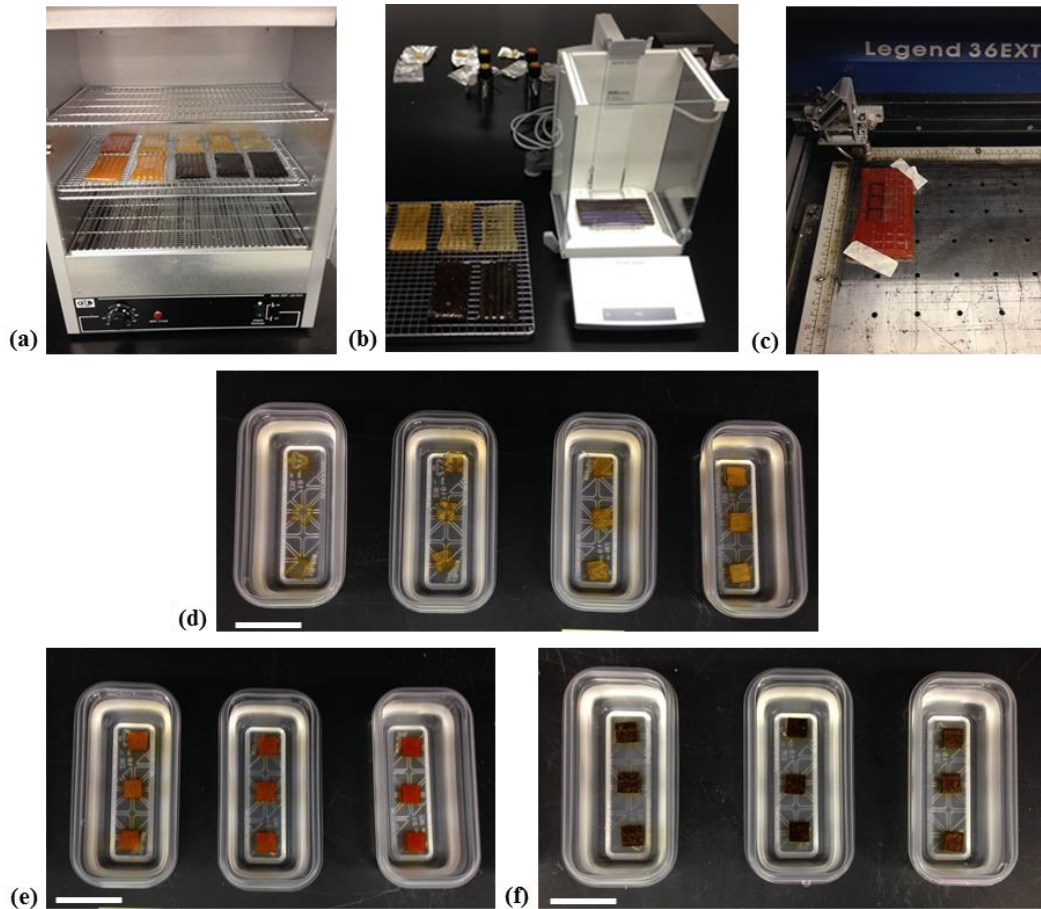


Figure 25: Moisture absorption test process (a) specimens placed in oven (b) specimens weighed to determine weight loss (c) 15mm x 15mm squares laser cut (d) from left to right, 10%, 20%, 30%, and 40% g/w specimens (5cm scale bar) (e) from left to right, 0.25%, 0.5%, and 1% TPA/g added to 40% g/w specimens (5cm scale bar) (f) from left to right, 2.5%, 5%, and 10% T/g added to 40% g/w specimens (5cm scale bar).

The weights of the specimens were measured at subsequent time intervals until an equilibrium was reached or the specimen degraded. The moisture content, MC, was calculated according to the following equation:

$$MC = \frac{W_t - W_0}{W_0} \times 100\% \quad \text{Eq. 20}$$

where W_t is the weight of the swollen sample at a certain time, and W_0 is the weight of the sample after any preconditioning. The dimensions of the dried (after preconditioning and before immersion in distilled water) and the swollen (immersed for 7 days) samples were measured to

obtain the change in volume. The dried specimens after preconditioning are shown in Figure 26a, and the fully swollen specimens are shown in Figure 26b.

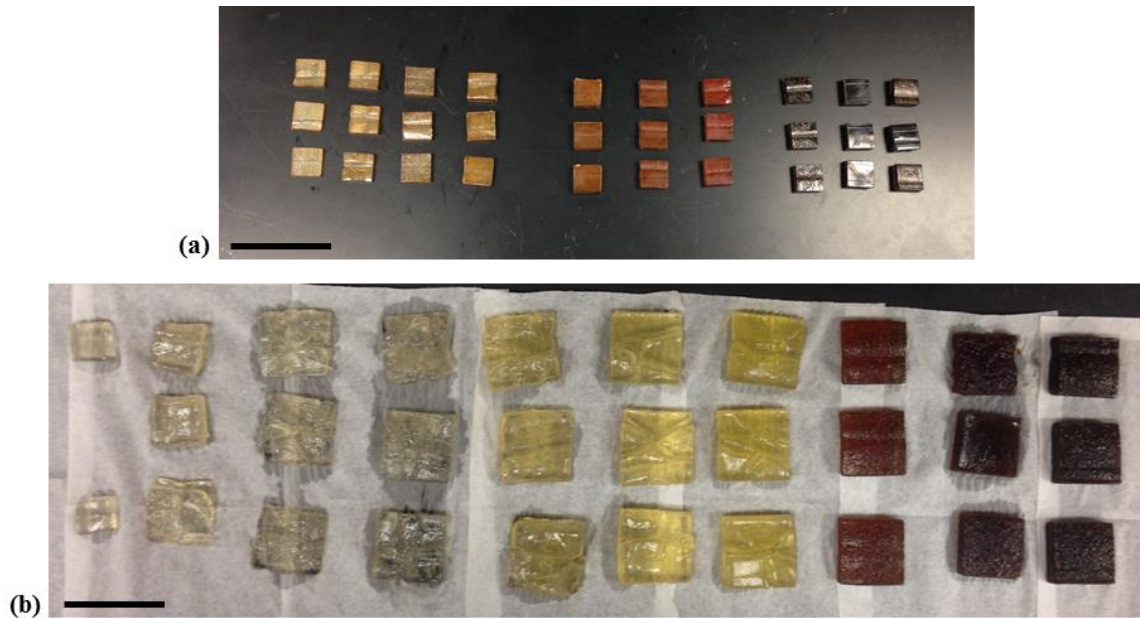


Figure 26: Moisture absorption specimens (a) dried (5cm scale bar) and (b) swollen (5cm scale bar), from left to right for both (a) and (b) 10%, 20%, 30%, and 40% g/w specimens followed by 0.25%, 0.5%, and 1% TPA/g added to 40% g/w specimens followed by 2.5%, 5%, and 10% T/g added to 40% g/w specimens.

3.2.13 Flexure Properties of GWV Composites Conditioned in High and Low Humidity

The effect of high and low humidity on flexural properties was determined for GWV composites made using 40% g/w resin with three (3) different cross-linking agents (none, T, and TPA). The preparation is further described in Section 3.2.6.2, and the different GWV composite groups will be referred to as G (40% g/w), T (40% g/w and 10% T/g), and TPA (40% g/w and 0.25% TPA/g). The G, T, and TPA GWV composites were cured in ambient conditions for 7 days. Flexure specimens for G, T, and TPA GWV composites were cut using a bandsaw to dimensions specified by ASTM D790. Three (3) unconditioned flexure specimens of G, T, and TPA GWV composites, respectively, were tested on day 7. The flexure specimens were tested as described in Section 3.2.11. Also on day 7, twelve (12) flexure specimens of G, T, TPA GWV composites were placed

in low humidity and high humidity chambers, respectively. The low humidity chamber was prepared by placing a supersaturated solution of commercial sodium chloride in a sealed plastic container. The high humidity chamber was prepared by placing a supersaturated solution of sodium phosphate in a sealed plastic container. The sealed plastic containers were 59.9cm x 45.5cm x 20.1cm weathertight storage boxes from IRIS USA, Inc. The temperature and humidity in each chamber was recorded using an EL-USB-2-LCD temperature and humidity data logger from Lascar Electronics. For the low humidity chamber, the data logger recorded an average relative humidity of 77.05% with a standard deviation of 1.79% and an average temperature of 22.5°C with a standard deviation of 0.74°C. For the high humidity chamber, the data logger recorded an average relative humidity of 102.6% with a standard deviation of 2.66% and an average temperature of 22.9°C with a standard deviation of 0.74°C. All the specimens were placed on grates in the chamber to ensure full exposure to the humidity condition. Figure 27a shows the flexure specimens in the low humidity chamber, while Figure 27b shows the flexure specimens in the high humidity chamber. Three (3) flexure specimens of G, T, and TPA GWV composites were tested on 1, 3, 7, and 14 days of being in their respective chambers. The flexure specimens were tested as described in Section 3.2.11.

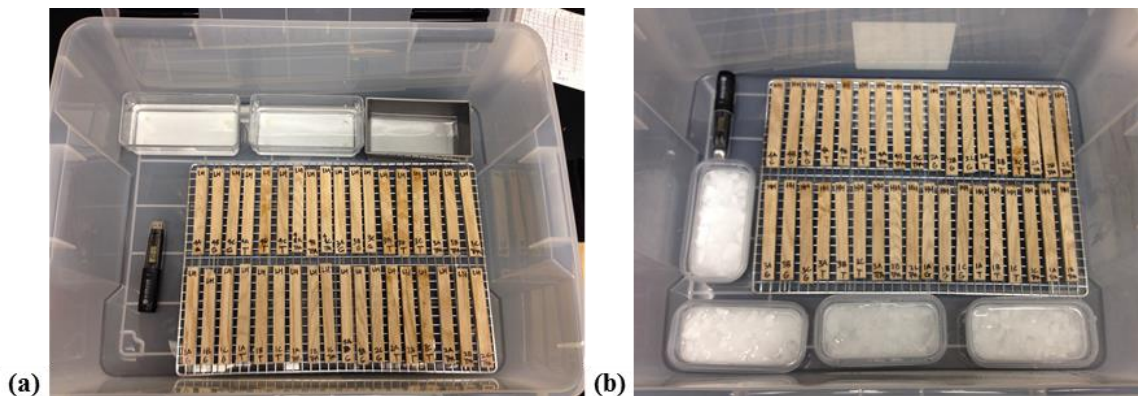


Figure 27: GWV composite flexure specimens in (a) low humidity and (b) high humidity chambers.

CHAPTER 4

RESULTS AND DISCUSSION

4.1 Gelatin Resin

4.1.1 *Tensile Mechanical Properties of Gelatin*

4.1.1.1 Stress-Strain Response

The stress-strain response of the gelatin film samples with varying gelatin content to weight of water (g/w ratio) is shown in Figure 28. The results show that, while all samples exhibited similar stress-strain relationships, the elongation-to-break increased with g/w content from 10% to 40%. While the 10% g/w samples remained linear elastic before rupture, the 20%, 30%, and 40% g/w samples exhibited an increasingly plastic response. The improved ductility may be attributed to the presence of random coils in the gelatin network. Random coils are more amorphous than the helical structures which may allow for more elongation before failure, as shown in Figure 28. It is suggested that as gelatin concentration increases the network becomes more entangled and, consequently, the growth of helical structures slows and more random coils remain in the network [Djabourov 2013]. Although there is improved ductility, the gelatin films still exhibit predominately brittle behavior in the dried state which may be attributed to the rigid chain nature of the biopolymer. As water leaves the gelatin polymer network during curing, large internal stresses develop from gelatin contraction [Kozlov 1983]. The variable response, namely the higher g/w ratios of 30% and 40%, may be due to greater internal stresses because of an increase in gelatin concentration and, therefore, contraction. The increasing occurrence of gelatin contraction may cause inconsistent distribution of internal stresses and lead to variability. The development of

internal stresses seems to depend on the curing conditions. For example, reduced internal stresses were observed in gelatin films cured at 0% relative humidity [Kozlov 1983].

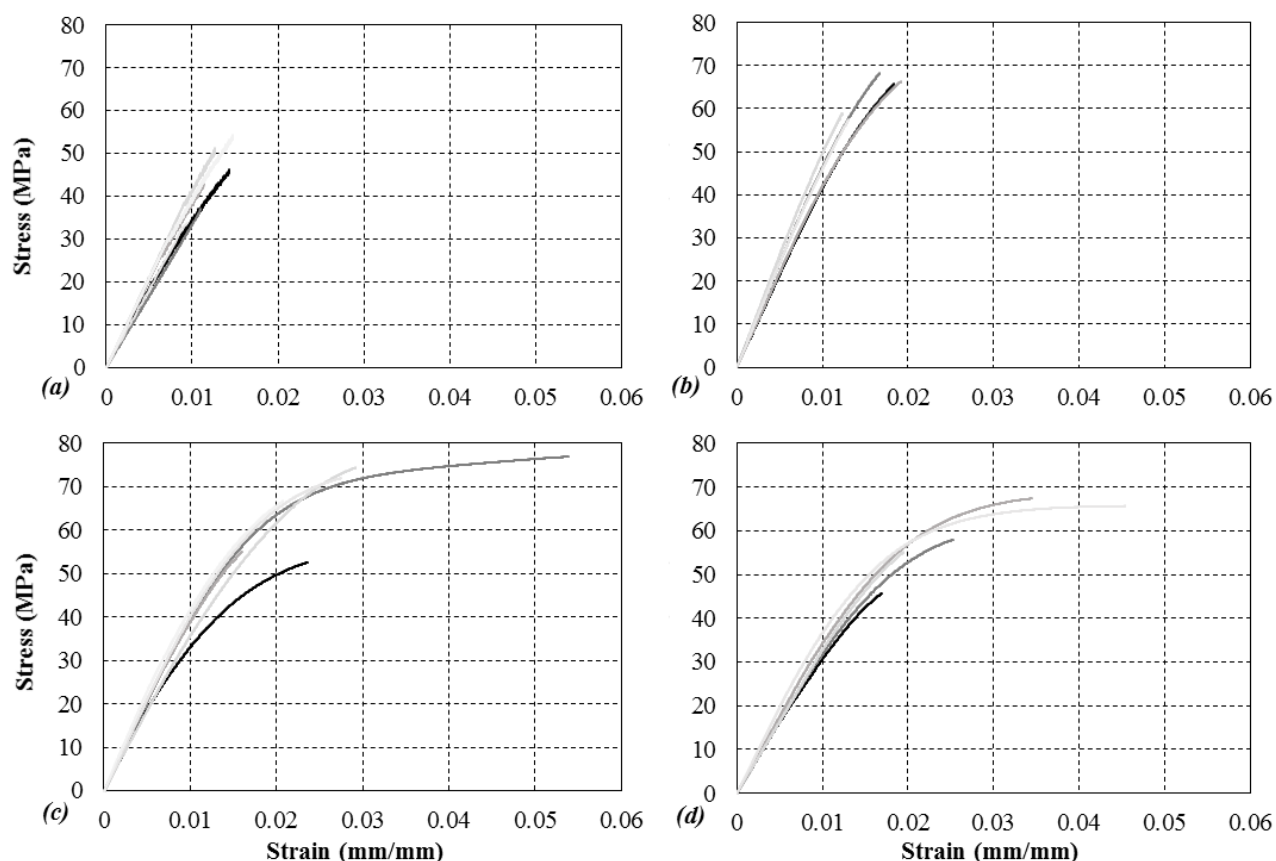


Figure 28: Stress-strain curves for gelatin films with (a) 10% g/w (b) 20% g/w (c) 30% g/w and (d) 40% g/w where the colors represent different specimens.

4.1.1.2 Tensile Strength and Elastic Moduli

The tensile strengths and moduli of the gelatin films are shown in Figure 29. According to the data, the tensile strength and modulus reached average maximum values of 66.3 MPa and 4728 MPa at 30% and 20% g/w content, respectively. Confirmation of the statistically significant difference between the mechanical property mean results from the varied gelatin concentration films was completed using an ANOVA analysis, as shown in Table 1. If the p-values are less than 0.05, the mean values are statistically different from each other and highlighted in Table 1. For maximum tensile strength, 20%, 30%, and 40% g/w content have comparable mean values according to the

ANOVA analysis. A notable peak, however, can be observed for the 30% g/w content. For tensile modulus, 20% g/w content has the greatest mean value according to the ANOVA analysis. There is a statistically significant decreasing trend in the mean value after 20% g/w content, but 30% g/w content demonstrates a sufficient mean tensile modulus. Therefore, the data suggest a favorable 30% ratio of water to gelatin that maximizes mechanical strength and stiffness while considering elongation-to-break. In addition, the 30% g/w resin tensile strength and modulus exceed their respective ACI 440.8-13 the minimum requirements for FRP saturating resins, as further described in Section 4.1.1.4. Given the experimental mechanical property results and the ACI 440.8-13 minimum requirements, a 30% g/w resin was chosen for continued analysis of gelatin-based FRP composites.

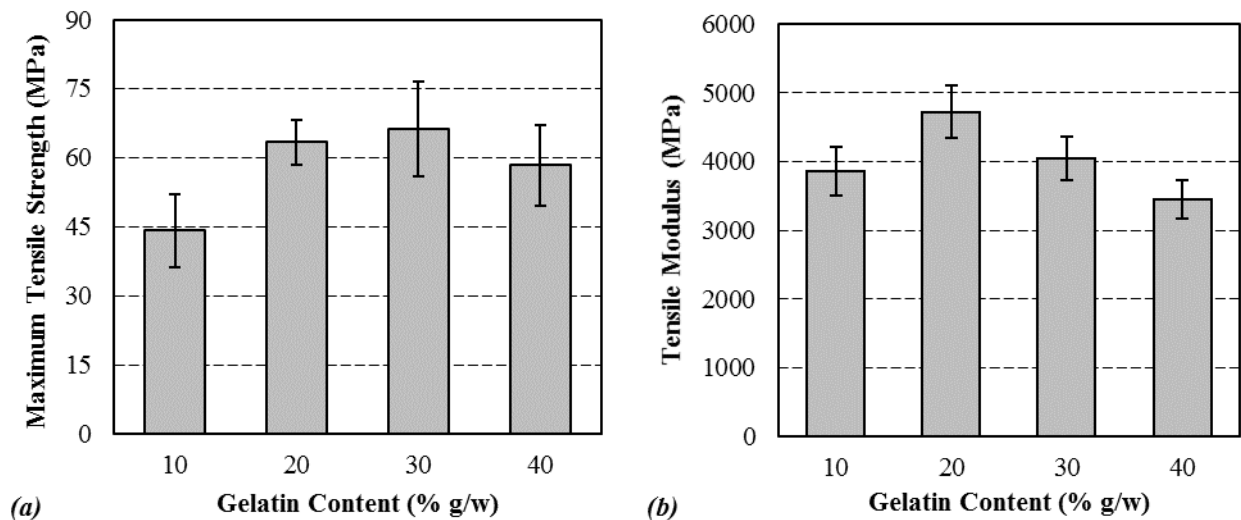


Figure 29: Tensile properties of gelatin films (a) strength and (b) modulus.

Table 1: ANOVA results for tensile strength and modulus of gelatin films

Mechanical Property	Gelatin Concentration		p-value
	Selected	Compared to	
Maximum Tensile Strength	10%	20%	0.0011
		30%	0.0019
		40%	0.0204
	20%	30%	0.569
		40%	0.297
		40%	0.205
Tensile Modulus	10%	20%	0.0034
		30%	0.343
		40%	0.0640
	20%	30%	0.0110
		40%	0.00031
		40%	0.0095

A previous study considered gelatin resin as a biobased wood adhesive and tested the breaking strength by applying a coat of gelatin resin to adhere two wood substrate surfaces subsequently subjecting the specimen to tensile loading. Gelatin resins with 5%, 10%, 20%, 30%, 40%, and 50% g/w ratios were tested. The results showed the highest average breaking strength of 7.5 MPa occurred when the gelatin resin had a g/w ratio of 40% [Dorr 2015]. Although there is a decrease in tensile mechanical properties as the g/w ratio of the gelatin resin increases from 30% to 40%, the maximum tensile strength and tensile modulus of the 40% g/w resin remain at acceptable values. In addition to the experimental data, Kim and Netravali (2013) suggest the sizeable amount of hydroxyproline present in gelatin creates additional hydrogen bonds when in contact with the cellulose on surface of the wood substrate resulting in increased strength of the adhesive assembly. The 40% g/w resin was chosen for continued analysis of engineered wood composites due to its optimal breaking strength performance with wood substrates, acceptable tensile mechanical properties, and the suspected gelatin-cellulose interaction.

4.1.1.3 Effect of Curing Time 30% g/w Films

Figure 30 shows the changes in mechanical properties of the 30% g/w films that occurred over a curing period of 21 days. Both tensile strength and elastic modulus increased over time with an average increase of approximately 96% and 21% from 3 to 21 days, respectively. The data is plotted on a logarithmic scale to show the relationship between time and mechanical property development. The changes in both strength and stiffness properties exhibited approximate linear relationships on a logarithmic scale as denoted by the coefficient of determination, R^2 . These data suggest that the mechanical properties of the gelatin films may continue to gain in mechanical strength and stiffness beyond 21 days. The increasing tensile modulus compares to a study conducted by Dai and Liu (2006) in which the tensile modulus of gelatin films also increased with time from approximately 4.0 GPa to 5.5 GPa. This trend may be attributed to increased crystallinity of the gelatin films. A similar shift in mechanical properties with physical aging is also found for some synthetic glassy amorphous polymers annealed below their glass transition temperature [Dai 2006].

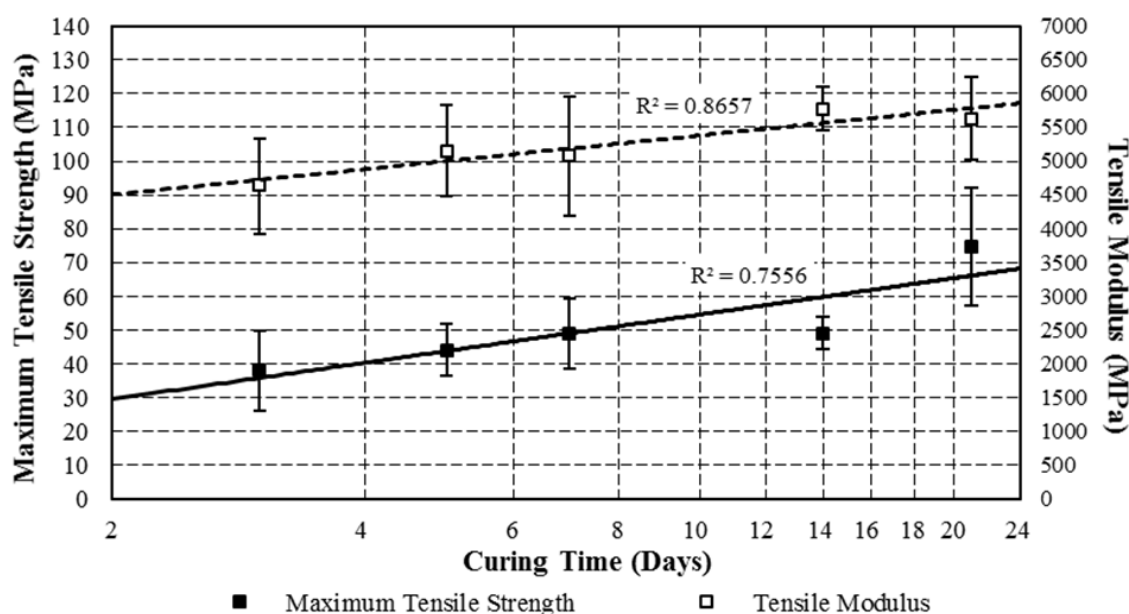


Figure 30: Tensile strength and modulus of 30% gelatin by weight films over time.

4.1.1.4 Comparison of Mechanical Testing to American Concrete Institute (ACI) Code

The 30% g/w resin selected to develop the FRP composite was compared to the applicable ACI code. The current standard design requirements for FRP materials made by wet layup for external strengthening of concrete and masonry structures are determined by ACI 440.8-13. The experimentally determined tensile strengths, tensile moduli, and elongation to break of gelatin resins are shown in Figure 31a, Figure 31b, and Figure 31c, respectively. The figures also compare the tensile properties of the gelatin resins to the respective minimum tensile properties of saturating resins according to ACI 440.8-13. The minimum tensile properties for saturating resins are reported in Table 7.1.2 of ACI 440.8-13 and provided in Table 2 with conversions from English to metric units, for reference.

Table 2: Minimum properties for saturating resins (ACI 440.8-13)

Property	ASTM test method	Mean value	
Ultimate tensile strength	D638 Type I	6000 psi	41.4 MPa
Tensile modulus	D638 Type I	250,000 psi	1724 MPa
Elongation at failure	D638 Type I	0.03	

According to the data, the tensile strength peaked at 30% g/w and reached a maximum value of 66.3 MPa, as shown in Figure 31a. The 30% g/w resin also significantly exceeded the ACI 440.8-13 minimum tensile strength for saturating resins by 60%. All of the tested gelatin resins exceeded the ACI 440.8-13 minimum ultimate tensile strength requirement, but the 30% g/w resin had the highest average maximum tensile strength. Figure 31b shows the tensile modulus peaked at 20% g/w and reached a maximum value of 1728 MPa. All of the tested gelatin resins exceeded the ACI 440.8-13 minimum tensile modulus, but the 20% and 30% g/w resins exceeded the requirement by 174% and 135%, respectively

According to the data, the elongation-to-break peaked at 40% g/w and reached a maximum value of 0.0289 mm/mm, as shown in Figure 31c. The standard deviation shows comparability to the 30% g/w resin and there is only a 3.7% difference between the average elongation at failure for 30% and 40% g/w resins. Although the tested gelatin resins did not exceed the ACI 440.8-13 minimum elongation at failure, the average elongation at failure for the 30% and 40% g/w resins were only 7% and 4% lower, respectively. In addition, the standard deviations for the 30% and 40% g/w resins exceed the ACI 440.8-13 minimum requirement which shows the potential for gelatin resins to be developed to satisfy the initial mechanical requirements.

Above 30% g/w, a notable decrease in mechanical properties was observed for both the tensile strength and modulus. The notable peaks in tensile strength and modulus suggest an optimal ratio of water to gelatin that maximizes mechanical strength and stiffness. In addition, the 30% g/w resin showed improved elongation at failure when compared to lower gelatin concentration resins. Given these results, the 30% by weight gelatin resin was chosen for continued analysis in developing biobased FRP composites.

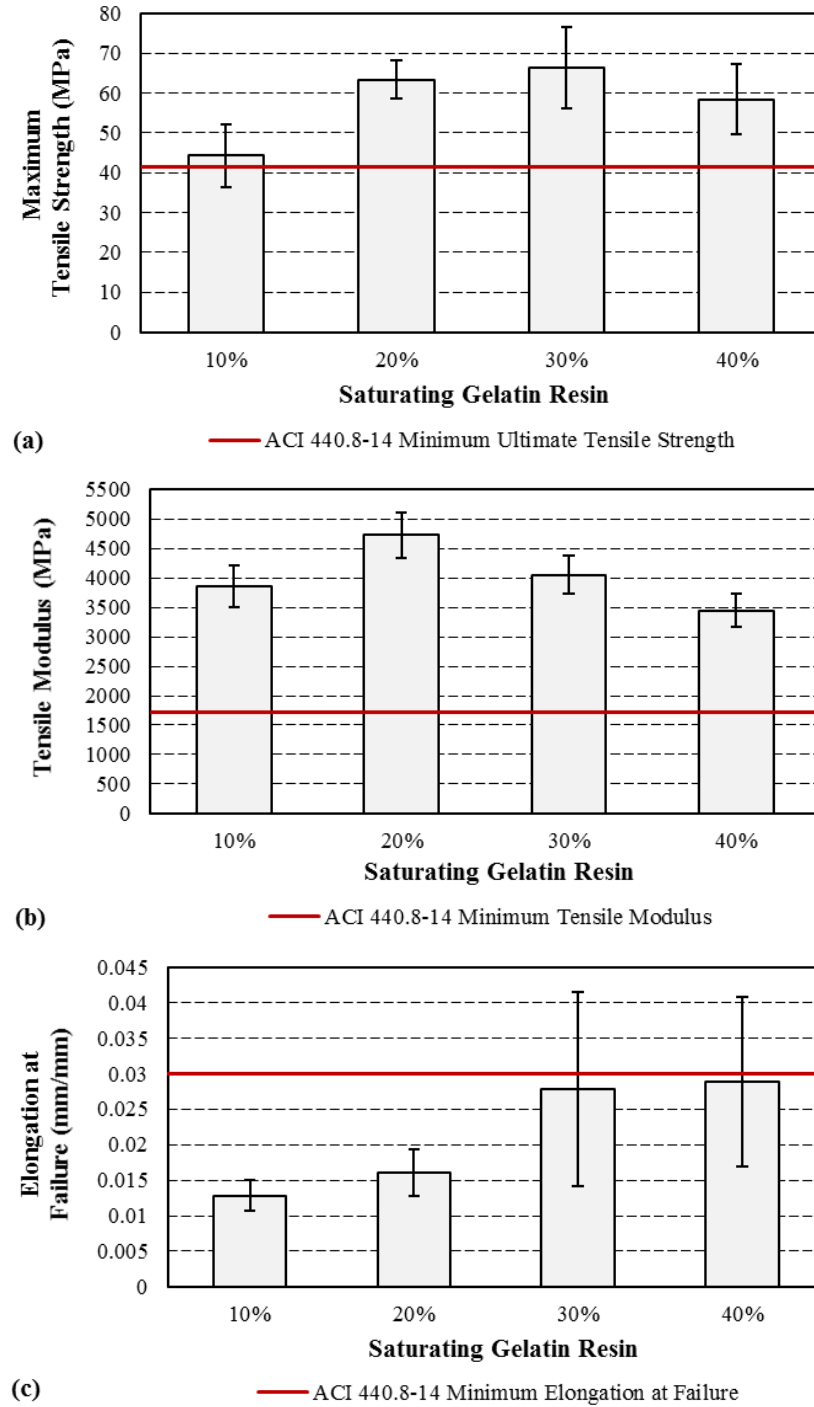


Figure 31: Tensile properties of gelatin saturating resins with comparison to ACI 440.8-13 (a) maximum tensile strength (b) tensile modulus and (c) elongation at failure.

4.1.2 *Moisture Absorption Properties of Gelatin and Cross-linked Gelatin Resins*

4.1.2.1 Moisture Absorption Properties of Gelatin Resins

Figure 32 shows the moisture contents of gelatin resins (10%, 20%, 30%, and 40% g/w) completely immersed in DI water over 10 days. The data is plotted versus the square root of the time to show the relationship between time and the absorption of water into the gelatin polymer network. Square-root-time was used as the metric since diffusion, in this case water, is well known to exhibit a square-root-time dependence. As expected, the gelatin resins absorbed water until reaching an approximate equilibrium point. The 10% g/w resin absorbed the most amount of water and reached an average equilibrium moisture content of 1636%. One (1) of the 10% g/w samples degraded and could not be measured on the 10th day, so the final measurement is based on two (2) samples. The 20% and 30% g/w resin reached average equilibrium moisture contents of 1029% and 1034%, respectively. The 40% g/w resin absorbed the least amount of water and reached an average equilibrium moisture content of 1006%. Although 20%, 30%, and 40% g/w content have a comparable average equilibrium moisture contents, the 40% g/w content consistently absorbs less water at each time interval. When compared to 10% g/w content resins, 40% g/w absorbed 38.5% less water over 10 days. The data suggest that 40% g/w content has the greatest resistance to water absorption, and was therefore chosen as the best performing gelatin content to use with cross-linking agents (e.g., wine tannin and terephthalaldehyde).

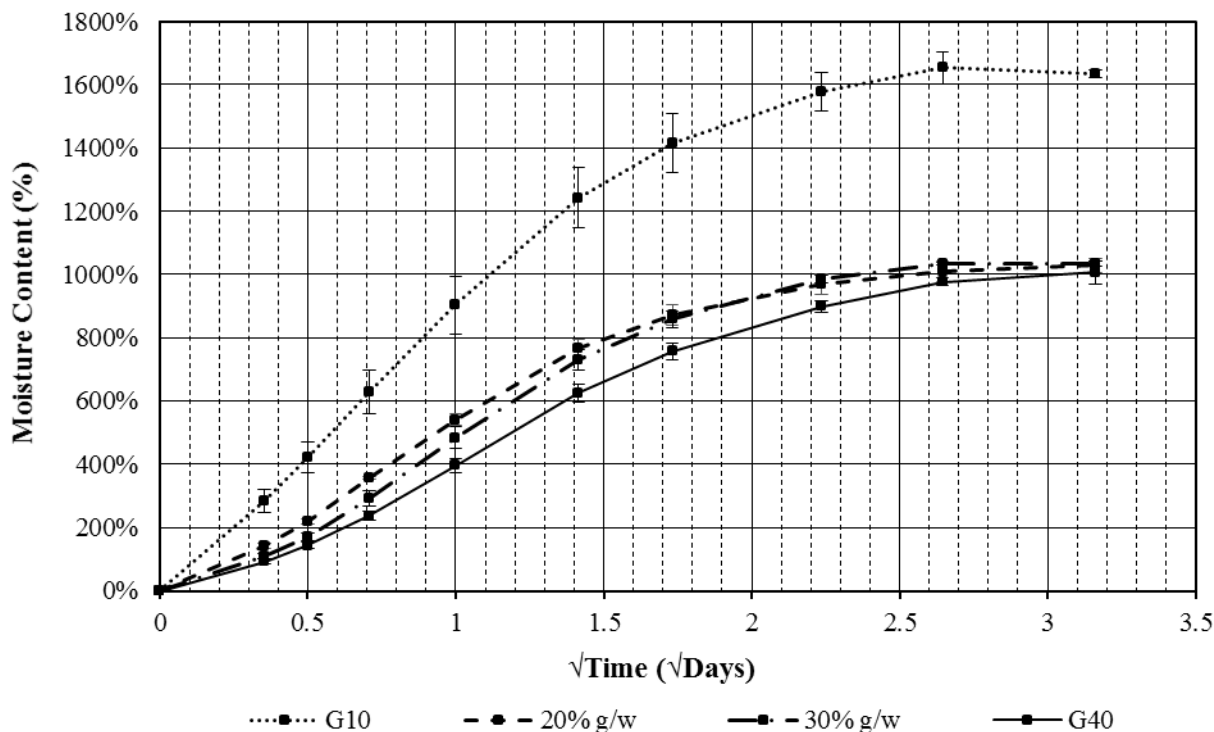


Figure 32: Moisture content for gelatin resins.

As the concentration of gelatin increases, the degree of moisture absorption decreases, as shown in Figure 32, especially before 2.5 $\sqrt{\text{days}}$. Increasing the concentration has been attributed to an increasingly entangled network [Djabourov 2013]. The denser network may prevent the absorption of water resulting in reduced moisture content for higher gelatin concentrations.

4.1.2.2 Moisture Absorption Properties of Cross-linked Gelatin Resins

Figure 33 shows the moisture content of 40% g/w resin compared to 40% g/w resin with wine tannin (T) and terephthalaldehyde (TPA) cross-linking agents. For TPA cross-linked gelatin resins, ratios of 0.25%, 0.5%, and 1% TPA to gelatin (TPA/g) by weight are shown. For T cross-linked gelatin resins, ratios of 2.5%, 5%, and 10% T to gelatin (T/g) by weight are shown. The data is plotted versus square-root-time to show the relationship between time and the absorption of water into the gelatin-based polymer network. Square-root-time was used as the metric since diffusion,

in this case water, is well known to exhibit a square-root-time dependence. The 40% g/w resin absorbed the most amount of water and reached an average equilibrium moisture content of 1006%. All the cross-linked gelatin resins absorbed less water. The 0.25%, 0.5%, and 1% TPA/g cross-linked gelatin resins had comparable equilibrium moisture contents of 991%, 981%, and 994%, respectively. Although the 0.5% TPA/g resin had the least equilibrium moisture content, the 0.25% TPA/g resin absorbed the least amount of water of the TPA cross-linked gelatin resins for the first three (3) days. The 2.5%, 5%, and 10% T/g cross-linked gelatin resins had decreasing equilibrium moisture contents of 849%, 805%, and 698%, respectively, as the wine tannin content increased. The 10% T/g resin consistently absorbed less water at each time interval when compared to T/g cross-linked gelatin resins and all the other tested resins, as shown in Figure 33. When compared to 40% g/w content resins, 0.25% TPA and 10% T/g absorbed 8.3% and 34.8% less water, respectively, over 2 days and 1.5% and 30.6% less water, respectively, over 10 days. The data suggest that, of the TPA cross-linked gelatin resins, the 40% g/w with 0.25% TPA/g has the best early resistance to water, and the 40% g/w with 10% T/g content resin has the greatest resistance to water absorption of all gelatin-based resins. Based on the results, the 0.25% TPA/g and 10% T/g were chosen as the best performing cross-linked gelatin resins for continued analysis of the gelatin wood veneer (GWV) composites.

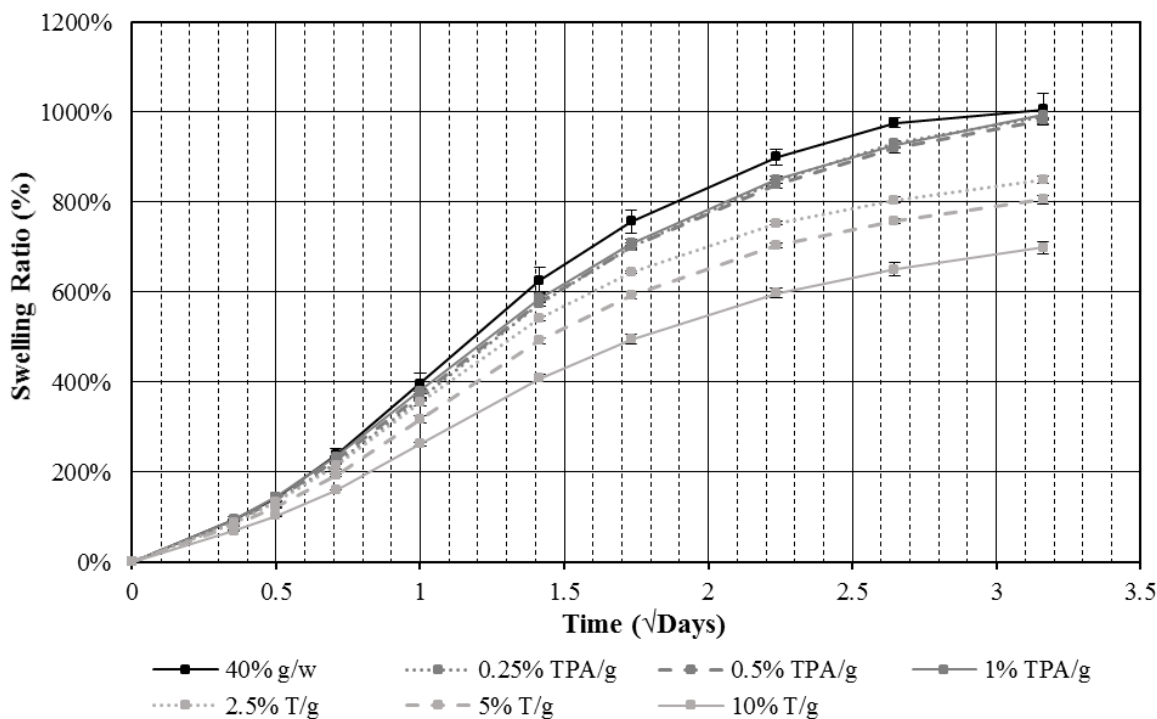


Figure 33: Moisture content for 40% g/w and cross-linked 40% g/w gelatin resins.

Table 3 shows the dried (initial) and swollen (final) volumes of the 40% g/w and 40% g/w cross-linked with TPA and T samples. Table 3 also provides the percent increase from the initial to final volume. The results show that cross-linking reduces the change in volume due to water absorption of gelatin-based resins. For TPA cross-linked 40% g/w resins, 0.25% TPA/g addition had the least amount of volume change and 137% less volume change when compared to uncross-linked 40% g/w resin. For T cross-linked 40% g/w resins, 10% T/g addition had the least amount of volume change and 563% less volume change when compared to uncross-linked 40% g/w resin. The T cross-linked 40% gelatin resins, especially 10% T/g, demonstrated the greatest resistance to moisture absorption as evident by the least amount of volume change. The improved resistance to moisture may be attributed to the formation of bonds between the tannin and gelatin molecules [Peña 2010]. Tannin is also known as a replacement for phenols in phenol-formaldehyde, a common wood adhesive [Pizzi 2011]. A polycondensation reaction takes place between tannin

and formaldehyde reaction to harden the resin [Kim 2009]. Higher reactivity of tannin, as opposed to phenol, with formaldehyde reduces the emission of formaldehyde which is known to have negative health effects [Pizzi 2011]. The successful implementation of tannin in formaldehyde wood adhesives suggests that tannin is compatible with wood substrates and supports its use as a cross-linking agent for gelatin wood adhesives.

Table 3: Volume change for 40% g/w and cross-linked 40% g/w resins

Sample	Initial Volume (V_i) (cm^3)		Final Volume (V_f) (cm^3)		Percent Increase (from V_i to V_f)
	Average	Standard Deviation	Average	Standard Deviation	
40% g/w	0.80	0.061	10.91	0.297	1266%
0.25% TPA/g	0.89	0.008	10.96	0.290	1129%
0.5% TPA/g	0.85	0.025	11.41	0.423	1241%
1% TPA/g	0.88	0.016	11.41	0.423	1199%
2.5% T/g	0.79	0.030	8.47	0.080	973%
5% T/g	0.87	0.026	8.11	0.246	835%
10% T/g	1.03	0.013	8.30	0.184	703%

4.2 Epoxy Resin

4.2.1 Tensile Mechanical Properties

The mechanical properties, namely ultimate tensile strength, tensile modulus, and elongation to break, of the epoxy resin are shown in Table 4, along with the 7-day mechanical properties of the gelatin films. The epoxy exhibits both a lower tensile strength and a lower tensile modulus compared to the gelatin resins, while the elongation-to-break of the epoxy is comparable to the gelatin films. Specifically, the maximum tensile strength and tensile modulus achievable by the gelatin films were 133% and 107% higher than the epoxy resin, respectively. For comparison, Bai (2013) reports ranges for tensile mechanical properties as 28 to 91 MPa for tensile strength, 2.4 to 4.5 GPa for tensile modulus, and 2 to 6% for elongation to break.

Table 4: Mechanical properties of resins

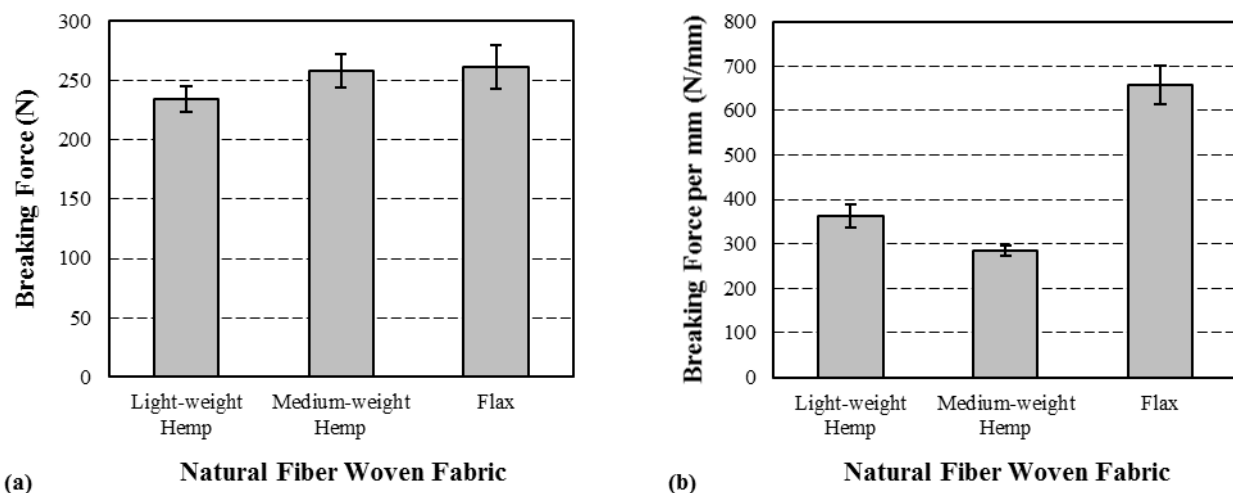
Resin	Maximum Tensile Strength (MPa)			Tensile Modulus (MPa)			Elongation-to-Break (mm/mm)		
	Mean	Standard Deviation	Coefficient of Variation	Mean	Standard Deviation	Coefficient of Variation	Mean	Standard Deviation	Coefficient of Variation
10% Gelatin	44.2	7.9	17.9%	3858	352	9.1%	0.0128	0.0022	16.8%
20% Gelatin	63.3	4.8	7.6%	4728	381	8.1%	0.0161	0.0033	20.8%
30% Gelatin	66.3	10.2	15.4%	4052	322	8.0%	0.0278	0.0137	49.1%
40% Gelatin	58.3	8.8	15.0%	3445	283	8.2%	0.0274	0.0113	41.2%
Epoxy	28.4	5.6	19.6%	1961	142	7.3%	0.0199	0.0051	25.4%

4.3 Woven Fabric

4.3.1 Breaking Force Properties of Light-weight Hemp, Medium-weight Hemp, and Flax

The breaking force and breaking force per mm of thickness of three (3) different woven natural fiber fabrics are shown in Figure 34a and Figure 34b, respectively. The average breaking force of light-weight hemp, medium weight hemp, and flax was 234.6 N, 258.0 N, and 261.6 N, respectively. The percent difference between light-weight hemp and flax was only 11% which shows that the natural fiber fabrics have similar resistance to applied force. For comparison, the breaking force of synthetic non-alkali glass fabric ranges from 490 to 2450 N and 255 to 1570 N in the warp and weft directions, respectively. The variable range is perhaps due to the grade of glass fiber [Wang 2011].

When the thickness of the fabric is considered, as shown in Figure 34b, the flax fabric demonstrated the strongest breaking force per mm of thickness with an average of 658.5 N/mm. When compared to light-weight hemp and medium-hemp, flax exhibited a higher breaking force per mm by 82% and 132%, respectively. Given these mechanical property results, flax woven natural fiber fabric was chosen for continued analysis of FRP composites.



(a) Natural Fiber Woven Fabric **(b)** Natural Fiber Woven Fabric
 Figure 34: Mechanical properties of natural fiber woven fabric (a) breaking force and (b) breaking force per mm of thickness.

4.4 Fiber Reinforced Polymer (FRP) Composites

4.4.1 Tensile Mechanical Properties of G-Fl, G-Fi, E-Fl, and E-Fi

The fiber mass and volume fractions of the four (4) FRP composites (E-Fi, E-Fl, G-Fi, and G-Fl) were approximately 11%, 15%, 16%, and 16%, respectively, which corresponded to volume fractions of approximately 5%, 15%, 10%, and 5%, respectively.

The tensile strength and modulus of the four (4) FRP composites are shown in Figure 35a and Figure 35b, respectively. Confirmation of the statistically significant difference between the mechanical property mean results from the four (4) FRP composites was completed using an ANOVA analysis, as shown in Table 5. If the p-values are less than 0.05, the mean values are statistically different from each other and highlighted in Table 5. For maximum tensile strength, the fully biobased (G-Fl) composite has a comparable mean value to the fully synthetic composite (E-Fi), and the fully biobased (G-Fl) and fully synthetic (E-Fi) composites have mean values that are statically higher than the partially biobased composites (E-Fl, G-Fi). For tensile modulus, the fully biobased composite (G-Fl) has the greatest statistically significant mean value according to the ANOVA analysis.

As shown in Figure 35a, the fully synthetic (E-Fi) and fully biobased (G-Fi) composites exhibited higher tensile strengths than the partially biobased composites (E-Fi, G-Fi). For example, the tensile strength of the fully synthetic E-Fi composites was 123% higher than the partially biobased E-Fi composites. Similarly, the tensile strength of the fully biobased G-Fi composite was 52% higher than the partially biobased G-Fi composites. The fully biobased G-Fi composites exhibit a tensile strength only 12% less than the fully synthetic E-Fi composite. The improved tensile strength for the E-Fi and G-Fi composites may be attributed to an improved interfacial bond between the compatible fully synthetic and the fully biobased constituents.

The cohesiveness of the interface is well known to influence the tensile strength of natural fiber composites. Improved interfacial adhesion is expected in hydrophilic-hydrophilic and hydrophobic-hydrophobic fiber-matrix systems [George 2001]. The incompatibility of hydrophobic polymer resins with hydrophilic natural fibers is well acknowledged, and surface treatments are commonly used to strengthen interface compatibility [George 2001, Zhu 2013]. The results of this study suggest that the use of the hydrophilic gelatin resin may improve the interfacial adhesion with hydrophilic natural flax fibers resulting in better tensile mechanical properties without the use surface modification [Zhu 2013, Zhang 2013]. Thus, given that gelatin and flax are both hydrophilic and epoxy and fiberglass are both hydrophobic, the compatibility of the fiber-matrix interface may be better than hydrophilic-hydrophobic fiber-matrix systems. This compatibility may not be true for all fully biobased fiber-matrix systems. For example, gelatin is both hydrophilic and biobased, while other biopolymers (e.g., polylactic acid, polyhydroxybutyrate) have inherently hydrophobic chemistries [George 2001, Zhu 2013, Zhang 2013, Auras 2011]. When comparing the fully biobased and fully synthetic composites described

within the scope of this study, it is suggested that the improved interfacial adhesion is due to the fully hydrophobic or fully hydrophilic properties of the constituents.

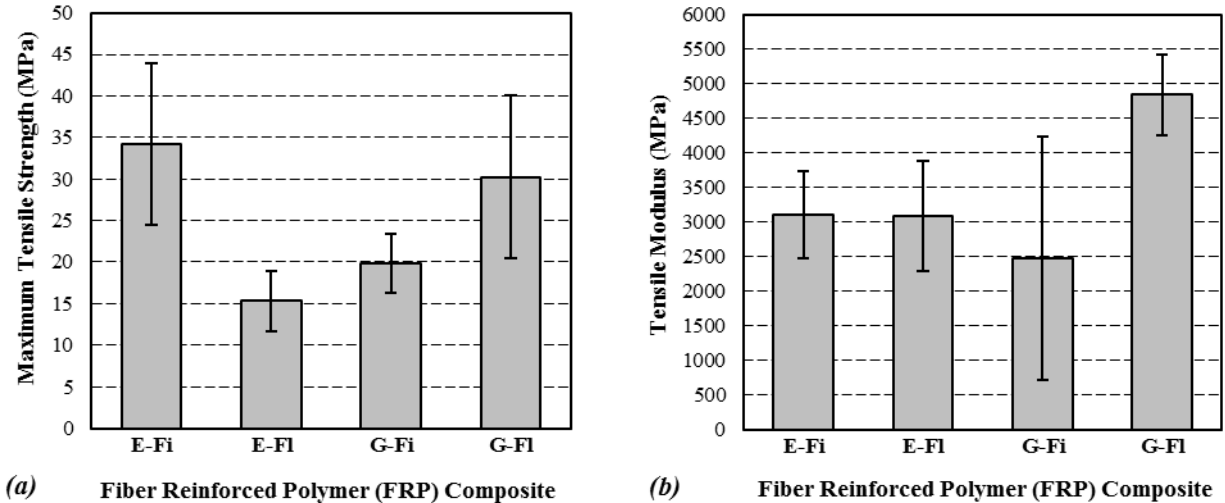


Figure 35: Tensile mechanical properties of FRP composites (a) strength and (b) modulus.

Table 5: ANOVA results for tensile strength and modulus of FRP composites

Mechanical Property	FRP Composite		p-value
	Selected	Compared to	
Maximum Tensile Strength	E-Fi	E-Fi	0.00042
		G-Fi	0.0018
		G-Fi	0.463
	E-Fi	G-Fi	0.0305
		G-Fi	0.0026
		G-Fi	0.0146
Tensile Modulus	E-Fi	E-Fi	0.961
		G-Fi	0.390
		G-Fi	0.00016
	E-Fi	G-Fi	0.418
		G-Fi	0.00050
		G-Fi	0.0048

In terms of composite stiffness, the average tensile modulus of the fully biobased G-Fi composites was 56% greater than the fully synthetic E-Fi composites, as shown in Figure 35b. For primary structural elements, fully biobased composites may not have suitable stiffness and strength for the application [Netravali 2014]. The promising results of gelatin flax for tensile strength and

especially tensile modulus demonstrate potential for the fully biobased composite to compete with its synthetic equivalent. For the epoxy-fiber composites, the average tensile modulus was approximately equal, regardless of reinforcement type. As expected, there is high variability in the data for the gelatin natural fiber composites. This effect can be attributed to the inherent variability of natural fibers and the variation in gelatin mechanical properties [Gioffre 2012, Arvanitoyannis 2002, Netravali 2015].

Huang and Netravali (2007) found that for FRP composites consisting of woven flax fiber within a soy protein concentrate (SPC) based resin matrix had mean tensile strengths of 54.6 MPa and 68.7 MPa and mean tensile moduli of 994 MPa and 1123 MPa for the warp and weft fiber direction, respectively [Huang 2007]. Compared to the flax and gelatin FRPs, the higher tensile strength may be attributed to the Huang and Netravali (2007) materials and methods, such as four (4) layers of flax fabric and temperature and pressure conditioning. The flax and gelatin FRPs, however, demonstrate greater tensile modulus than the flax and SPC FRPs. Kumar et. al. (2010) found that woven flax fiber within a polylactic acid (PLA) resin had a mean tensile strength of 21 MPa and a mean tensile modulus of 137 MPa [Kumar 2010]. The flax and gelatin FRPs had slightly a higher mean tensile strength and a significantly higher mean tensile modulus which may be attributed to the hydrophilic-hydrophilic compatibility between the gelatin and flax constituents. Flax as a natural fiber reinforcement for FRPs has been previously researched for many different polymer matrices [Zhu 2013, Yan 2014]. Flax and gelatin resin FRPs, however, are not well characterized, but demonstrate promising results, as indicated by this study.

4.4.2 Tensile Fracture Surface Morphology of G-Fl, G-Fi, E-Fl, and E-Fi

After mechanical testing, the fracture surfaces of the four (4) FRP composites were examined. The SEM micrographs of the fiber-matrix interface for E-Fl, E-Fi, G-Fi, and G-Fl specimens are shown

in Figure 36a – Figure 36d, respectively. It can be seen in Figure 36a and Figure 36c that the interfaces for E-Fi and G-Fi have a relatively weak bond as evident by the separation between the polymer matrix and fiber reinforcement. The fully synthetic (Figure 36b) and fully biobased composite (Figure 36d) appeared to exhibit an improved bond as evident by the contiguity of the polymer matrix and reinforcing fiber. The improved mechanical properties of the fully synthetic and fully biobased composites enhanced bond may be attributed to an enhanced fiber-matrix interface of these composite systems. The tensile mechanical properties and SEM images performed in this study further corroborate the findings within the literature that indicate the influence of the interface between the fiber and resin on the mechanical properties of FRP composites [Hollaway 2010, Ku 2011, George 2001, Zhu 2013]. Together with the mechanical property data, the SEM images suggest that fully biobased E-Fi composites exhibit a marked potential to be an environmentally viable alternative to conventional E-Fi FRP composites.

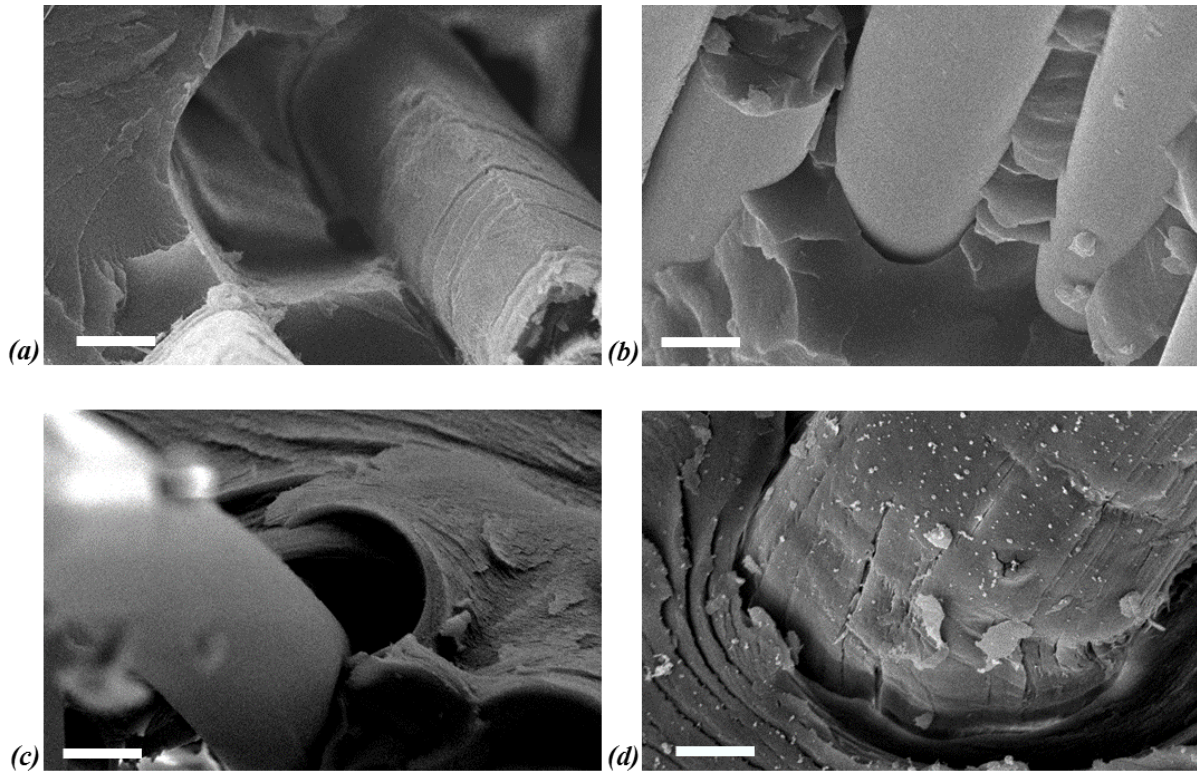


Figure 36: Scanning electron microscopy images of (a) E-Fi (5 μ m scale bar), (b) E-Fi (5 μ m scale bar), (c) G-Fi (5 μ m scale bar), and (d) G-Fi (5 μ m scale bar).

4.5 FRP Composite Strengthened Wood Beams

4.5.1 Flexural Mechanical Properties of Poplar Strengthened with One-Ply FRP Composite

The flexural strength and modulus of unreinforced poplar and four (4) different FRP composite strengthened poplar beams are shown in Table 6 and Table 7, respectively. The FRP composites include epoxy and fiberglass (E-Fi), epoxy and flax (E-Fi), 30% g/w resin and fiberglass (G-Fi), and 30% g/w resin and flax (G-Fi). Schematics of the flexural test setup and the cross-section of the FRP strengthened wood poplar beams are shown in Figure 37a and Figure 37b, respectively. The results provided in Table 6 and Table 7 show that the poplar wood has the greatest strength within the cross-section. This indicates that the mechanical properties of the reinforcement do not enhance the mechanical properties of the poplar wood. Table 7 shows that the average tensile stress in the (4) FRP composite materials within the cross-section ranges from 27.0 MPa (G-Fi) to 54.2

MPa (G-FI). Since the tensile stress of the FRP composite material is less than the average flexural stress of the unreinforced poplar, 117.2 MPa, the FRP reinforcement would not enhance the tensile capacity and therefore not improve the flexural strength. In order to improve the flexural strength of pristine wood beams, the FRP composites would need improved mechanical properties. This may be achieved by means such as increasing the number of plies or adjusting the fiber mass or volume fractions. The FRP composites may be better suited to improve the properties of deteriorated and weakened wood beams instead of pristine wood beams with full strength. The results motivated the application of gelatin-based resins for wood composites (e.g., GWV composites).

Table 6: Flexural mechanical properties for unreinforced poplar beam specimens

	Flexural Stress (MPa)		Flexural Modulus (MPa)	
	Average	Standard Deviation	Average	Standard Deviation
Unreinforced Poplar	117.2	5.3	12794	549

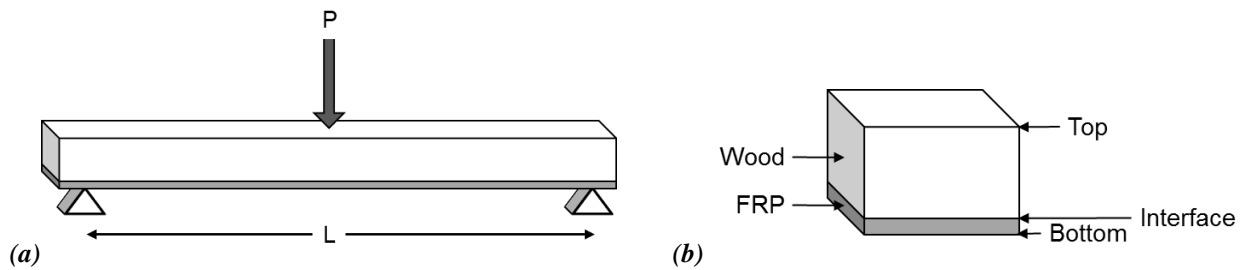


Figure 37: FRP composite specimen (a) flexural set-up and (b) cross-section.

Table 7: Flexural mechanical properties of FRP strengthened poplar wood beam specimens

FRP Reinforcement	<i>Top</i>		<i>Interface</i>				<i>Bottom</i>		Flexural Modulus (MPa)	
	Compressive Stress in Wood (MPa)		Tensile Stress in Wood (MPa)		Tensile Stress in FRP (MPa)		Tensile Stress in FRP (MPa)			
	<i>Average</i>	<i>Standard Deviation</i>	<i>Average</i>	<i>Standard Deviation</i>	<i>Average</i>	<i>Standard Deviation</i>	<i>Average</i>	<i>Standard Deviation</i>	<i>Average</i>	<i>Standard Deviation</i>
Epoxy-Fiberglass	146.9	3.8	133.0	3.4	32.2	3.8	44.5	1.2	15238	391
Epoxy-Flax	144.3	10.2	122.2	10.9	29.4	2.6	47.8	2.9	14690	637
Gelatin-Fiberglass	126.6	7.4	123.3	6.6	23.9	1.3	27.0	2.0	12261	473
Gelatin-Flax	127.2	6.8	116.4	5.5	44.0	2.1	54.2	3.4	12817	530

4.6 Gelatin-based Wood Veneer (GWV) Composites

4.6.1 Flexural Mechanical Properties

The flexural strength and modulus of gelatin wood veneer (GWV) composites and conventional engineered wood products are shown in Figure 38 and Figure 39, respectively. The GWV composites contain (1) hardwood species as the wood veneer with 40% g/w resin and (2) softwood species as the wood veneer with 40% g/w resin. For comparison, the conventional engineered wood products include oriented strand board (OSB), medium density fiberboard (MDF), and plywood. Of the conventional engineered wood products shown, plywood has the greatest average flexural strength and modulus with values of 38.2 MPa and 7.75 GPa, respectively. The average flexural strength of hardwood and softwood GWV composites is 197% and 209% higher than plywood, respectively. The average flexural modulus for the GWV composites is comparable to plywood. Hardwood GWV composites have a 13% higher and softwood GWV composites have a 5% lower average flexural modulus when compared to plywood. The data suggest that GWV composites may compete with conventional plywood for certain applications.

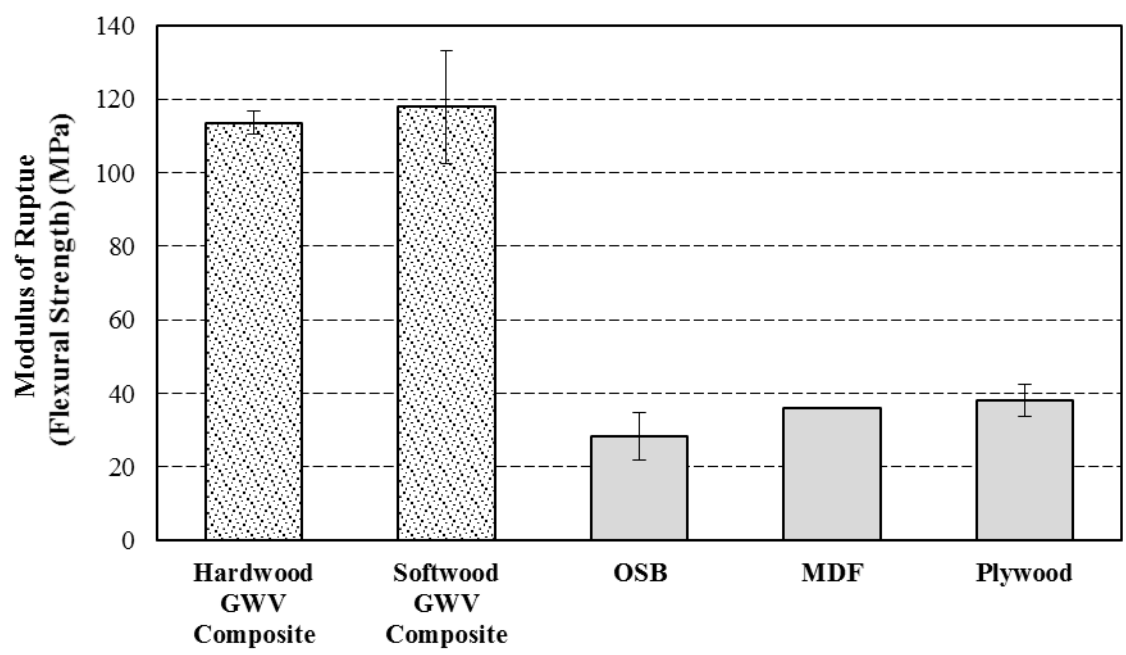


Figure 38: Flexural strength for gelatin based and conventional engineered wood.

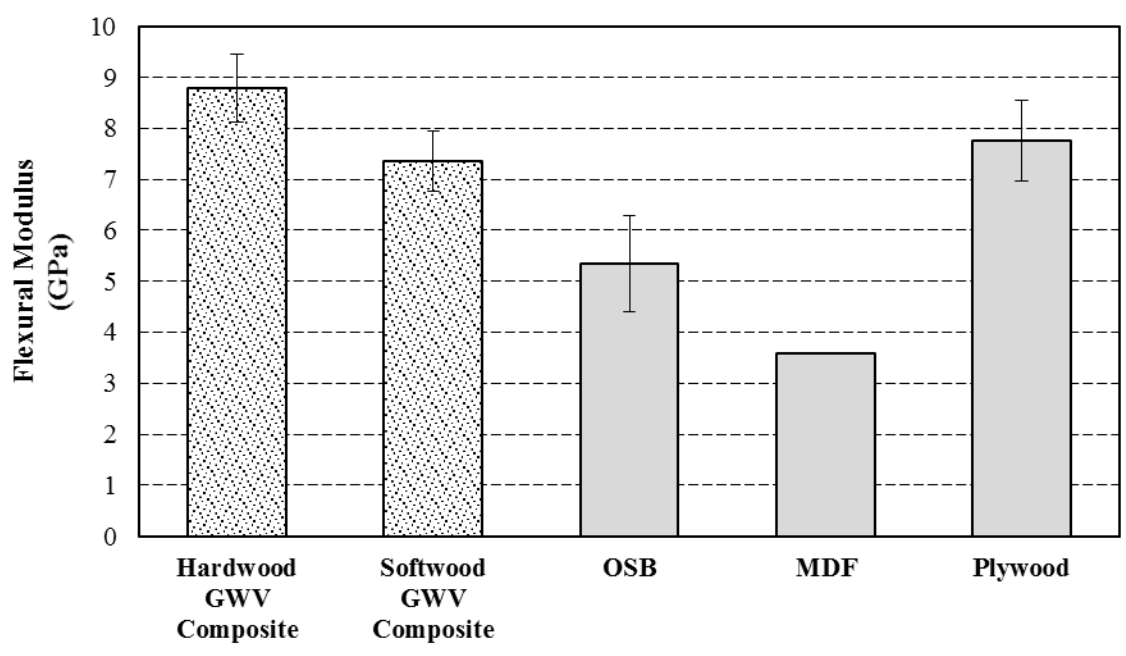


Figure 39: Flexural modulus for gelatin based and conventional engineered wood.

4.6.2 Cost Comparison of GWV Composites to Conventional Engineered Wood

The Figure 40 shows a cost comparison between the GWV composites and conventional engineered wood products based on a square foot. The unit prices for the GWV composites were estimated using the material costs incurred for fabrication [Knox 2015, Woodcraft 2015]. An average wood veneer thickness was measured using calipers. Since there were 8 plies, the thickness of the combined wood veneer was subtracted from the total thickness of the wood composite to determine the amount of gelatin. The material cost of one square foot was then estimated since the amount of each constituent was approximately known. It was assumed that the amount of water remaining in the gelatin resin after curing was negligible. The unit prices for OSB, MDF, and plywood were estimated based on commercial vendor sale prices [Home Depot 2015, Lowes 2015]. The cost comparison provides a preliminary investigation of the economic feasibility of GWV composites. Since the laboratory cost is within an order of magnitude of the manufactured cost, there is potential for GWV composites to be economically competitive as an alternative to conventional wood panels. In addition, the cost is represented per square foot and the GWV composites demonstrate improved flexural properties and may require less material, and therefore less cost, than conventional wood panels.

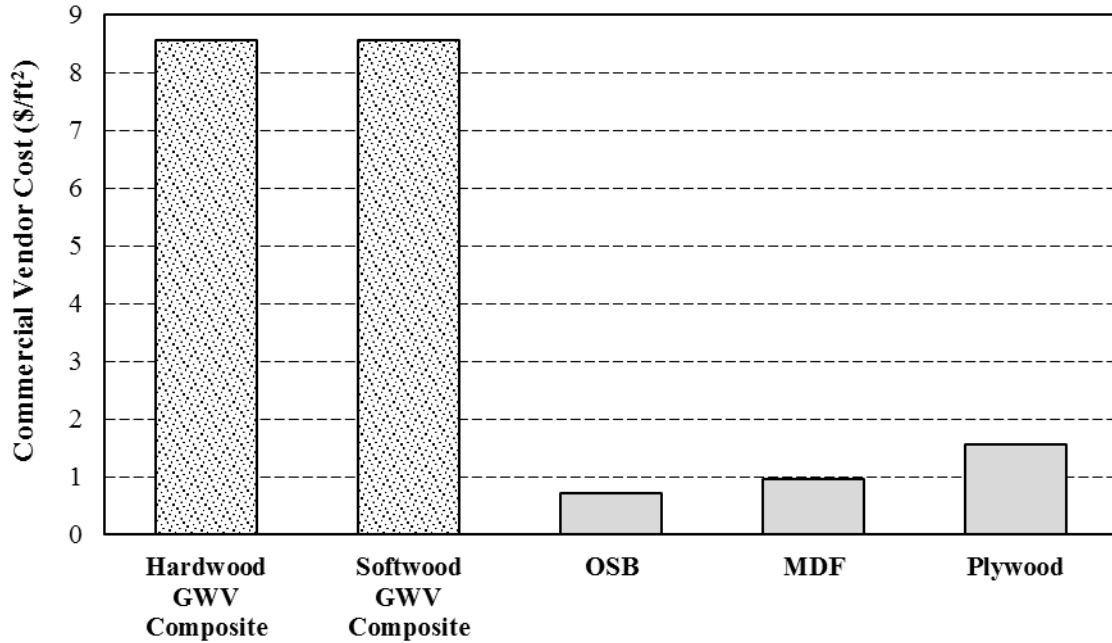


Figure 40: Cost comparison of gelatin based and conventional engineered wood.

4.6.3 Flexural Properties of GWV Composites in High and Low Humidity Conditions

Figure 41 and Figure 42 show the change in flexural properties over time of GWV composites made using 40% g/w resin with and without cross-linking agents in low and high humidity conditions, respectively. The low and high humidity conditions are shown in Table 8, for reference.

Table 8: Conditions in low and high humidity chambers

Humidity Condition	Relative Humidity (%)		Temperature (°C)	
	Average	Standard Deviation	Average	Standard Deviation
Low	77.05%	1.79%	22.5	0.74
High	102.6%	2.66%	22.9	0.74

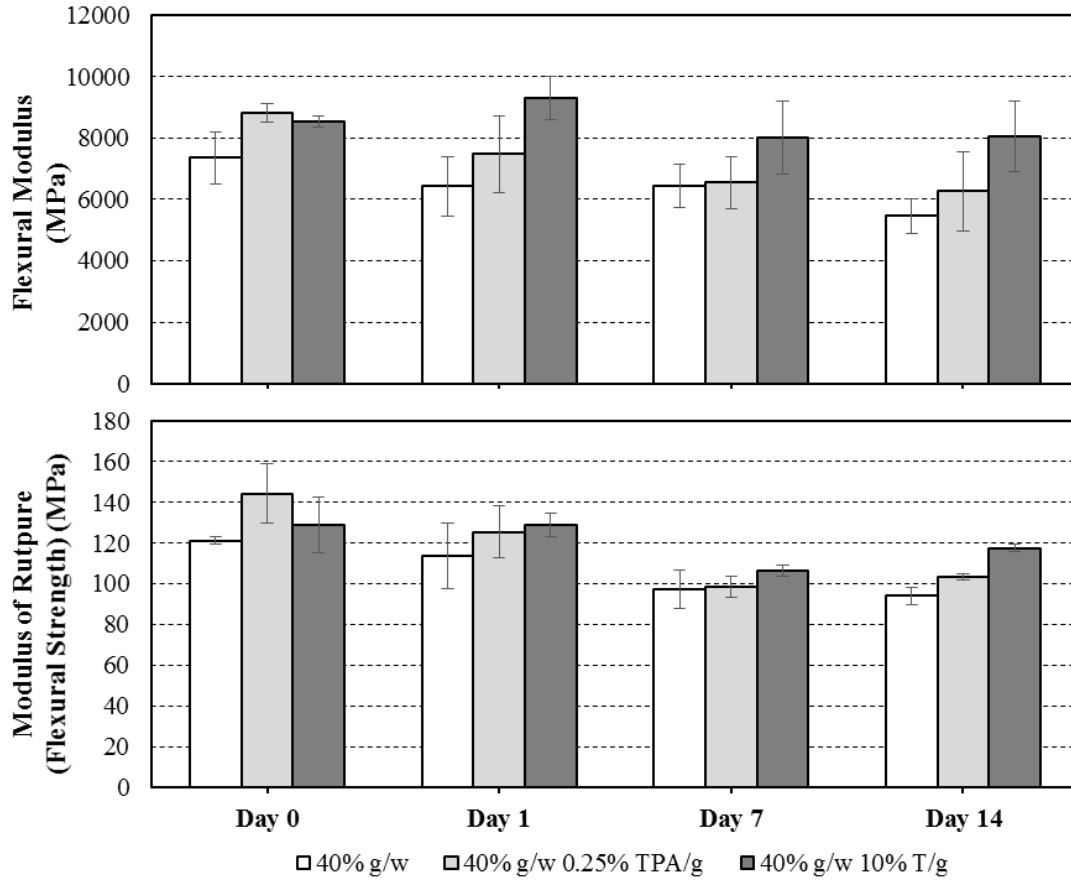


Figure 41: Flexural properties of oak GWV composites in low humidity conditions over time.

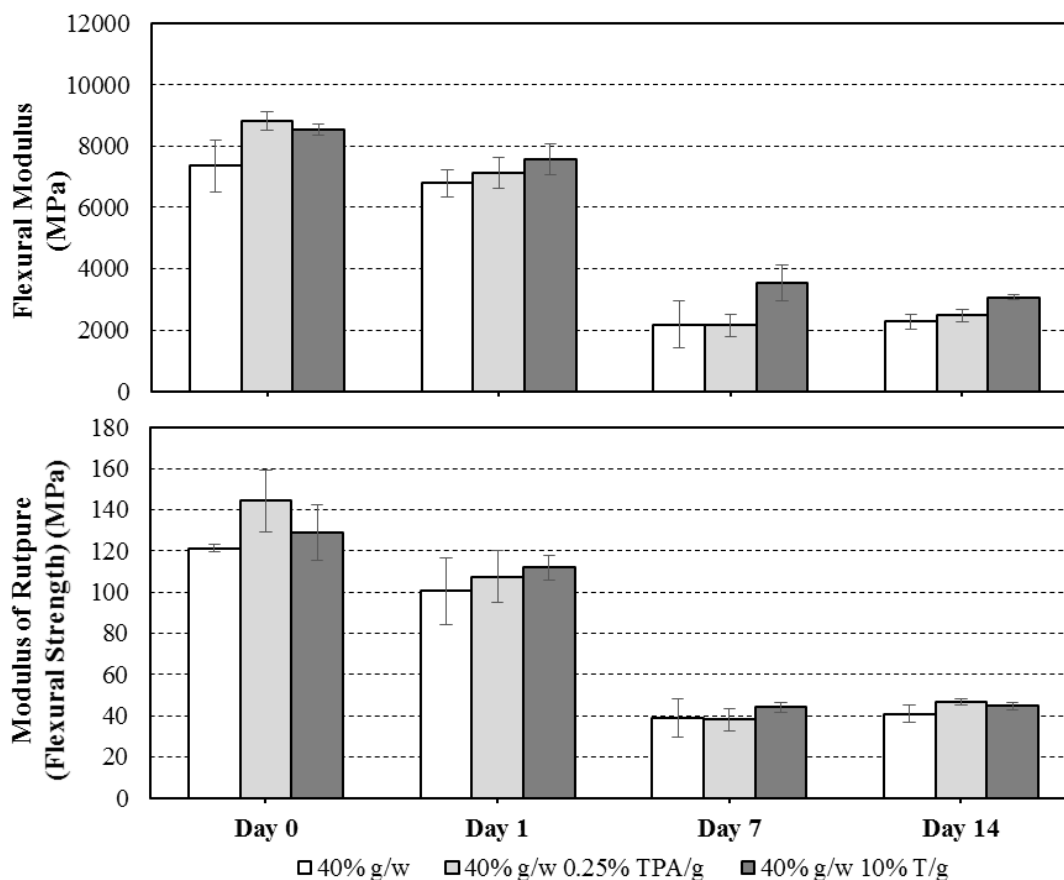


Figure 42: Flexural properties of oak GWV composites in high humidity conditions over time.

In low humidity conditions over 14 days, the 40% g/w resin GWV composites containing no cross-linking agent, 0.25% TPA/g, and 10% T/g exhibited reductions in flexural strength of 22%, 28%, and 9% and reductions in flexural modulus of 26%, 29%, and 6%, respectively. The GWV composites containing 40% g/w resin with 10% T/g cross-linking agent demonstrated the greatest resistance to deterioration in the low humidity environment. The data suggest the flexural properties of GWV composites can be maintained in low humidity environment.

In high humidity conditions over 1 day, the 40% g/w resin GWV composites containing no cross-linking agent, 0.25% TPA/g, and 10% T/g exhibited reductions in flexural strength of 17%, 26%, and 13% and reductions in flexural modulus of 8%, 19%, and 11%, respectively. In high humidity conditions over 7 days, the 40% g/w resin GWV composites containing no cross-

linking agent, 0.25% TPA/g, and 10% T/g exhibited reductions in flexural strength of 68%, 74%, and 66% and reductions in flexural modulus of 71%, 76%, and 59%, respectively. It can be observed that the GWV composites maintained sufficient flexural properties over a 1 day period, but lost significant capacity over a 7 day period. The GWV composites containing 40% g/w resins with 10% T/g cross-linking agent performed better than the GWV composites containing 40% g/w resins with 0.25% TPA/g. Overall, the study showed that GWV composites, especially containing 40% g/w resin with 10% T/g, maintained flexural properties in low humidity conditions, but lost flexural properties after 1 day in high humidity conditions.

CHAPTER 5

CONCLUSIONS

The study successfully achieved its intended purpose. (1) The 10%, 20%, 30%, and 40% g/w resins demonstrated tensile mechanical properties that exceeded the tensile strength and modulus minimum requirements provided in ACI 440.8-14. (2) Moisture absorption tests showed that gelatin-based resins prepared with terephthalaldehyde and wine tannin effectively improved the moisture resistance. (3) The gelatin based resin proved most effective as a biobased adhesive in a novel gelatin wood veneer (GWV) composite. Compared to commercially available wood panels (e.g., OSB, MDF, and plywood), the GWV composite had significantly greater flexural strength and demonstrated a similar average flexural modulus as plywood. GWV composites also showed the potential to be cost competitive as a biobased alternative to conventional wood panels. In addition to achieving the purpose of the study, other conclusions about the gelatin-based resins, FRP composites, and GWV composites can be drawn from results.

5.1 Gelatin-Based Resins

The tensile mechanical properties of 10%, 20%, 30%, and 40% g/w resins and moisture absorption properties of gelatin resins with and without additives were investigated. The results indicated the following conclusions:

1. 30% gelatin-to-water (g/w) films have improved tensile properties (i.e., strength, elastic modulus, elongation-to-break) when compared to conventional epoxy resins
2. 30% g/w films gain strength and stiffness up to 21 days and may continue to do so as the indicated by the respective approximate linear relationships of the data on a logarithmic scale.

3. 30% and 40% g/w films exceed the minimum tensile strength and modulus requirements in ACI 440.8-13 for saturating resins.
4. 40% g/w absorbed the least amount of water when compared to 10%, 20%, and 30% g/w.
5. Moisture absorption properties were shown to improve when T and TPA were added to gelatin resins. Of the tested resins, 40% g/w resin with 10% T/g addition demonstrated the greatest resistance to moisture.

5.2 Gelatin-Based FRP Composites Compared to Synthetic-Based FRP Composites

The tensile mechanical properties and fracture surface morphology of E-Fi, E-Fl, G-Fi, and G-Fl FRP composites were investigated. The (4) FRP composites were then used to strengthen poplar beams and tested to obtain flexural mechanical properties. The results indicated the following conclusions:

1. Fully biobased gelatin-flax composites exhibited comparable strength and enhanced stiffness compared to fully synthetic epoxy-fiberglass composites. In addition, composites with fully synthetic or fully biobased constituents demonstrated improved tensile properties when compared to composites with a combination of biobased and synthetic constituents.
2. The strength of gelatin-flax composites is influenced by the cohesiveness of the interface between the constituents, as indicated by SEM microscopy. It is suggested that the hydrophilic chemistries of the biobased constituents and the hydrophobic chemistries of the synthetic constituents may improve the interfacial adhesion and, therefore, the tensile mechanical properties.

3. The FRP composite, as tensile reinforcement, does not have enough tensile strength to enhance the flexural capacity and would not improve the flexural properties, as indicated by the results.
4. The FRP composites may be better suited to improve the properties of deteriorated and weakened wood beams instead of pristine wood beams with full strength.

5.3 Gelatin Wood Veneer (GWV) Composites

The flexural mechanical properties of GWV composites made using gelatin, gelatin-TPA, and gelatin-T resins were investigated. The flexural properties of GWV composites with 40% g/w resins kept in ambient conditions were compared to conventional wood panel products. Then, the GWV composites were contained in low humidity and high humidity conditions to determine the effect of gelatin resin cross-linking methods on the flexural properties over time. The results indicated the following conclusions:

1. The average flexural strength of GWV composites is greater than conventional wood panel products (e.g., OSB, MDF, and plywood), and the average flexural modulus is similar to that of plywood. The results suggest viability of GWV composites as a biobased alternative to wood panel products for certain applications.
2. The laboratory cost of GWV composites is within an order of magnitude of the cost of manufactured wood products. Therefore, there is potential for GWV composites to be economically competitive compared to conventional wood panels.
3. When conditioned in high and low humidity chambers, GWV composites, especially composites containing 40% g/w resin with 10% T/g, maintained flexural properties after 14 days in low humidity, but lost flexural properties after 1 day in high humidity.

CHAPTER 6

FUTURE WORK

The direction of the research described in this study may be summarized by providing future work opportunities for gelatin-based resins, gelatin based FRP composites, and GWV composites.

The continued investigation of gelatin-based resins for construction composites may be completed as follows. First, determine the tensile mechanical properties (e.g. tensile strength and stiffness) of cross-linked gelatin films. This study reported the tensile mechanical properties of gelatin films, but future research may determine the tensile mechanical properties of cross-linked gelatin films with TPA and T through mechanical testing and analysis. Second, improved water resistance may occur by increasing the ratio of TPA and T addition. Third, the degree of cross-linking and cross-link density may be determined through techniques such as differential scanning calorimetry or rheology tests. Finally, the helical content of the gelatin-based films may be determined through x-ray diffraction analysis or differential scanning calorimetry.

The future work to improve the gelatin-based FRP composites may be completed as follows. First, the FRP composite could be prepared and tested with multiple plies may improve the mechanical properties of the material. Biaxial mechanical test methods could also be implemented to further characterize the FRP composites. Additionally, the plies could be pressed during fabrication which may enhance the fiber-resin interface and also improve the properties by more effectively transferring load from the resin matrix to the fiber reinforcement. Finally, additional investigation into the interfacial properties may be conducted using mechanical test methods such as single fiber pull out tests.

The future work to improve the gelatin wood veneer (GWV) composites may be completed

as follows. First, incorporating pressure and/or heat into the preparation process may improve the adhesion between the gelatin resin and wood substrate and the consistency of the cross-section. Second, the plies of veneer could be oriented in different directions and tested in multiple loading scenarios for tailored properties and to support its potential application as a wood panel alternative. Finally, the GWV composite flexural specimens could be exposed to wet and dry cycles and mechanically tested to determine the changes in flexural properties over time.

REFERENCES

- Aboudi, J., Arnold, S. M., & Bednarczyk, B. A. (2012). *Micromechanics of composite materials: a generalized multiscale analysis approach*. Butterworth-Heinemann.
- ACI Committee 440, "Specification for Carbon and Glass Fiber-Reinforced Polymer (FRP) Materials Made by Wet Layup for External Strengthening of Concrete and Masonry Structures (ACI 440.8-13)". American Concrete Institute, Farmington Hills, MI, 2013.
- Aguilera, A. (Ed.). (2013). *Research Developments in Wood Engineering and Technology*. IGI Global.
- Ahmed, E. M. (2015). Hydrogel: Preparation, characterization, and applications: A review. *Journal of Advanced Research*, 6, 105-121.
- Arvanitoyannis, I. S. (2002). Formation and properties of collagen and gelatin films and coatings. *Protein-based films and coatings*, 275-304.
- ASTM Standard C39, 1921 (2014), "Standard Test Method for Compressive Strength of Cylindrical Concrete Specimens," ASTM International, West Conshohocken, PA, 2014, DOI: 10.1520/C0039_C0039M-14A, www.astm.org.
- ASTM Standard D5035, 1990 (2011), "Standard Test Method for Breaking Force and Elongation of Textile Fabrics (Strip Method)," ASTM International, West Conshohocken, PA, 2010, DOI: 10.1520/D5035-11, www.astm.org.
- ASTM Standard D5229, 1992 (2014), "Standard Test Method for Moisture Absorption Properties and Equilibrium Conditioning of Polymer Matrix Composite Materials," ASTM International, West Conshohocken, PA, 2010, DOI: 10.1520/D5229_D5229M-14, www.astm.org.
- ASTM Standard D638, 1941 (2010), "Standard Test Method for Tensile Properties of Plastics," ASTM International, West Conshohocken, PA, 2010, DOI: 10.1520/D0638-10, www.astm.org.
- ASTM Standard D790, 1970 (2010), "Standard Test Methods for Flexural Properties of Unreinforced and Reinforced Plastics and Electrical Insulating Materials," ASTM International, West Conshohocken, PA, 2010, DOI: 10.1520/D0790-10, www.astm.org.
- Auras, R. A., Lim, L. T., Selke, S. E., & Tsuji, H. (Eds.). (2011). *Poly (lactic acid): synthesis, structures, properties, processing, and applications* (Vol. 10). John Wiley & Sons.
- Bai, J. (Ed.). (2013). *Advanced fibre-reinforced polymer (FRP) composites for structural applications*. Elsevier.

- Bakis, C., Bank, L. C., Brown, V., Cosenza, E., Davalos, J. F., Lesko, J. J., Machida, Rizkalla, S.H., & Triantafillou, T. C. (2002). Fiber-reinforced polymer composites for construction-state-of-the-art review. *Journal of Composites for Construction*, 6(2), 73-87.
- Barnett, C. L. (2007). Green Buildings: Benefits to Health, the Environment, and the Bottom Line. US Senate Environment and Public Works Committee Hearing, Washington, DC, May 15, 2007. *Healthy Schools Network, Inc.*
- Bigi, A., Borghi, M., Cojazzi, G., Fichera, A. M., Panzavolta, S., & Roveri, N. (2000). Structural and mechanical properties of crosslinked drawn gelatin films. *Journal of Thermal Analysis and Calorimetry*, 61(2), 451-459.
- Bigi, A., Panzavolta, S., & Rubini, K. (2004). Relationship between triple-helix content and mechanical properties of gelatin films. *Biomaterials*, 25(25), 5675-5680.
- Biscarat, J., Galea, B., Sanchez, J., & Pochat-Bohatier, C. (2015). Effect of chemical cross-linking on gelatin membrane solubility with a non-toxic and non-volatile agent: Terephthalaldehyde. *International journal of biological macromolecules*, 74, 5-11.
- Bourtoom, T. (2009). Edible protein films: properties enhancement. *International Food Research Journal*, 16(1), 1-9.
- Brigante, D. (2013). *New Composite Materials: Selection, Design, and Application*. Springer International Publishing AG.
- Cao, N., Fu, Y., & He, J. (2007). Preparation and physical properties of soy protein isolate and gelatin composite films. *Food Hydrocolloids*, 21(7), 1153-1162.
- Cheng, H. N., Dowd, M. K., & He, Z. (2013). Investigation of modified cottonseed protein adhesives for wood composites. *Industrial Crops and Products*, 46, 399-403.
- Chiou, B. S., Avena-Bustillos, R. J., Shey, J., Yee, E., Bechtel, P. J., Imam, S. H., Glenn, G.M. & Orts, W. J. (2006). Rheological and mechanical properties of cross-linked fish gelatins. *Polymer*, 47(18), 6379-6386.
- Chung, D. (2010). *Composite Materials: Science and Applications* (2nd ed.). Springer Science & Business Media, 2010.
- Dai, C. A., & Liu, M. W. (2006). The effect of crystallinity and aging enthalpy on the mechanical properties of gelatin films. *Materials Science and Engineering: A*, 423(1), 121-127.
- Dixit, M. K., Fernández-Solís, J. L., Lavy, S., & Culp, C. H. (2012). Need for an embodied energy measurement protocol for buildings: A review paper. *Renewable and Sustainable Energy Reviews*, 16(6), 3730-3743.
- Djabourov, M., Nishinari, K., & Ross-Murphy, S. B. (2013). *Physical gels from biological and synthetic polymers*. Cambridge University Press.

Doi, M. (2013). *Soft Matter Physics*. Oxford University Press.

Dorr, D.N., Traeger L.S., Frazier S.D., Hess K.M., & Srubar III, W.V. (2015) Bond Strength of Biodegradable Gelatin-based Wood Adhesives. Submitted to *Journal of Renewable Materials*, December 2014.

Duconseille, A., Astruc, T., Quintana, N., Meersman, F., & Sante-Lhoutellier, V. (2015). Gelatin structure and composition linked to hard capsule dissolution: A review. *Food Hydrocolloids*, 43, 360-376.

Elisseeff, J. (2008). Hydrogels: structure starts to gel. *Nature materials*, 7(4), 271-273.

Frihart, C. R. (2011). Wood adhesives: vital for producing most wood products. *Forest products journal*, 61(1), 4-12.

Gelatin Market Projected to Reach \$2.79 Billion. (2013). *Neutraceuticals World*, 16(8), 24.

George, J., Sreekala, M. S., & Thomas, S. (2001). A review on interface modification and characterization of natural fiber reinforced plastic composites. *Polymer Engineering & Science*, 41(9), 1471-1485.

Gioffrè, M., Torricelli, P., Panzavolta, S., Rubini, K., & Bigi, A. (2012). Role of pH on stability and mechanical properties of gelatin films. *Journal of Bioactive and Compatible Polymers*, 27(1), 67-77.

Hanani, Z. N., Roos, Y. H., & Kerry, J. P. (2014). Use and application of gelatin as potential biodegradable packaging materials for food products. *International journal of biological macromolecules*, 71, 94-102.

Hollaway, L. C. (2010). A review of the present and future utilisation of FRP composites in the civil infrastructure with reference to their important in-service properties. *Construction and Building Materials*, 24(12), 2419-2445.

Hollaway, L. C., & Teng, J. G. (Eds.). (2008). *Strengthening and rehabilitation of civil infrastructures using fibre-reinforced polymer (FRP) composites*. Elsevier.

Huang, X., & Netravali, A. (2007). Characterization of flax fiber reinforced soy protein resin based green composites modified with nano-clay particles. *Composites Science and Technology*, 67(10), 2005-2014.

Jang, Y., Huang, J., & Li, K. (2011). A new formaldehyde-free wood adhesive from renewable materials. *International Journal of Adhesion and Adhesives*, 31(7), 754-759.

Jones, R. T. (2004). *Gelatin: manufacture and physico-chemical properties* (pp. 23-60). Pharmaceutical Press: London, UK.

- Khan, M. A., Islam, T., Rahman, M. A., Islam, J. M., Khan, R. A., Gafur, M. A., Mollah, M.Z.I. & Alam, A. K. M. (2010). Thermal, mechanical and morphological characterization of jute/gelatin composites. *Polymer-Plastics Technology and Engineering*, 49(7), 742-747.
- Kim, J. T., & Netravali, A. N. (2013). Performance of protein-based wood bioadhesives and development of small-scale test method for characterizing properties of adhesive-bonded wood specimens. *Journal of Adhesion Science and Technology*, 27(18-19), 2083-2093.
- Kim, J. T., & Netravali, A. N. (2013). Performance of protein-based wood bioadhesives and development of small-scale test method for characterizing properties of adhesive-bonded wood specimens. *Journal of Adhesion Science and Technology*, 27(18-19), 2083-2093.
- Kim, S. (2009). Environment-friendly adhesives for surface bonding of wood-based flooring using natural tannin to reduce formaldehyde and TVOC emission. *Bioresource Technology*, 100(2), 744-748.
- Knox Unflavored Gelatin Powder, 16 Ounce -- 12 per case. (2015, April 22). Retrieved from Amazon: http://www.amazon.com/Knox-Unflavored-Gelatine-16-Pack/dp/B00FUOPRAE/ref=sr_1_11?ie=UTF8&qid=1429727936&sr=8-11&keywords=knox+gelatin
- Kozlov, P. V., & Burdygina, G. I. (1983). The structure and properties of solid gelatin and the principles of their modification. *Polymer*, 24(6), 651-666.
- Ku, H., Wang, H., Pattarachaiyakoop, N., & Trada, M. (2011). A review on the tensile properties of natural fiber reinforced polymer composites. *Composites Part B: Engineering*, 42(4), 856-873.
- Kumar, R., Yakabu, M. K., & Anandjiwala, R. D. (2010). Effect of montmorillonite clay on flax fabric reinforced poly lactic acid composites with amphiphilic additives. *Composites Part A: Applied Science and Manufacturing*, 41(11), 1620-1627.
- La Mantia, F. P., & Morreale, M. (2011). Green composites: A brief review. *Composites Part A: Applied Science and Manufacturing*, 42(6), 579-588.
- Lam, F. (2001). Modern structural wood products. *Progress in structural engineering and materials*, 3(3), 238-245.
- Lau, K. T., & Zhou, L. M. (2001). Mechanical performance of composite-strengthened concrete structures. *Composites Part B: Engineering*, 32(1), 21-31.
- Leick, S., Degen, P., Köhler, B., & Rehage, H. (2009). Film formation and surface gelation of gelatin molecules at the water/air interface. *Physical Chemistry Chemical Physics*, 11(14), 2468-2474.
- Lumber & Composites: Plywood. (2015, April 22). Retrieved from Home Depot: <http://www.homedepot.com/b/Lumber-Composites-Plywood/N-5yc1vZbqm7>

- Netravali, A. N., & Chabba, S. (2003). Composites get greener. *Materials today*,6(4), 22-29.
- Netravali, A. N., & Pastore, C. M. (2014). *Sustainable Composites: Fibers, Resins and Applications*. DEStech Publications, Inc.
- Onusseit, H. (2010). *Renewable (Biological) Compounds in Adhesives for Industrial Applications* (pp. 189-199). Springer Vienna.
- Peña, C., De la Caba, K., Eceiza, A., Ruseckaite, R., & Mondragon, I. (2010). Enhancing water repellence and mechanical properties of gelatin films by tannin addition. *Bioresource technology*, 101(17), 6836-6842.
- Phillips, G. O., & Williams, P. A. (Eds.). (2011). *Handbook of food proteins*. Elsevier.
- Pizzi, A. (1989). *Wood Adhesives: Chemistry and Technology* (Vol. 2). New York: CRC Press.
- Pizzi, A., & Mittal, K. L. (Eds.). (2011). *Wood adhesives*. CRC Press.
- Plywood, OSB & Specialty Panels. (2015, April 22). Retrieved from Lowes: http://www.lowes.com/Building-Supplies/Lumber/Plywood-OSB-Specialty-Panels/_/N-1z10t8h/pl?Ns=p_product_qty_sales_dollar|1#!
- Rowell, R. M. (Ed.). (2012). *Handbook of wood chemistry and wood composites*. CRC press.
- Soradech, S., Nunthanid, J., Limmatvapirat, S., & Luangtana-Anan, M. (2012). An approach for the enhancement of the mechanical properties and film coating efficiency of shellac by the formation of composite films based on shellac and gelatin. *Journal of Food Engineering*, 108(1), 94-102.
- Stevens, E. S. (2002). *Green plastics: an introduction to the new science of biodegradable plastics*. Princeton University Press.
- Thakur, V. K. (Ed.). (2013). *Green composites from natural resources*. CRC Press.
- Thakur, V. K., & Singha, A. S. (Eds.). (2015). *Surface Modification of Biopolymers*. John Wiley & Sons.
- U.S. DoE (2008). Energy efficiency trends in residential and commercial buildings. *US Department of Energy, Washington, DC Available at: http://apps1.eere.energy.gov/buildings/publications/pdfs/corporate/bt_stateindustry.pdf*.
- U.S. EPA (2009). Recover Your Resources: Reduce, Reuse, and Recycle Construction and Demolition Materials at Land Revitalization Projects. EPA-560-F-09-523.
- Wang, R. M., Zheng, S. R., & Zheng, Y. P. G. (2011). *Polymer matrix composites and technology*. Elsevier.

Wood & Project Materials: Veneer. (2015, April 22). Retrieved from Woodcraft:
<http://www.woodcraft.com/category/SU114-23/Veneer.aspx>

Yakimets, I., Paes, S. S., Wellner, N., Smith, A. C., Wilson, R. H., & Mitchell, J. R. (2007). Effect of water content on the structural reorganization and elastic properties of biopolymer films: a comparative study. *Biomacromolecules*, 8(5), 1710-1722.

Yakimets, I., Wellner, N., Smith, A. C., Wilson, R. H., Farhat, I., & Mitchell, J. (2005). Mechanical properties with respect to water content of gelatin films in glassy state. *Polymer*, 46(26), 12577-12585.

Yan, L., Chouw, N., & Jayaraman, K. (2014). Flax fibre and its composites—A review. *Composites Part B: Engineering*, 56, 296-317.

Zhang, N., Liu, H., Yu, L., Liu, X., Zhang, L., Chen, L., & Shanks, R. (2013). Developing gelatin–starch blends for use as capsule materials. *Carbohydrate polymers*, 92(1), 455-461.

Zhu, J., Zhu, H., Njuguna, J., & Abhyankar, H. (2013). Recent development of flax fibres and their reinforced composites based on different polymeric matrices. *Materials*, 6(11), 5171-5198.